UNIVERSIDAD DE SALAMANCA (USAL)

ESCUELA POLITÉCNICA SUPERIOR DE ÁVILA

DEPARTAMENTO DE INGENIERÍA CARTOGRÁFICA Y DEL TERRENO

ÁREA DE INGENIERÍA HIDRÁULICA

TESIS DOCTORAL

RIESGO SÍSMICO Y ANÁLISIS DINÁMICO

DE PRESAS ARCO-GRAVEDAD

Enrico Zacchei

Ávila, septiembre 2018

UNIVERSIDAD DE SALAMANCA (USAL), ESPAÑA

ESCUELA POLITÉCNICA SUPERIOR DE ÁVILA

DEPARTAMENTO DE INGENIERÍA CARTOGRÁFICA Y DEL TERRENO

en cotutela con

UNIVERSIDAD DE SÃO PAULO (USP), BRASIL

ESCUELA POLITÉCNICA DE SÃO PAULO

DEPARTAMENTO DE INGENIERÍA DE ESTRUCTURAS Y GEOTECNIA

TESIS DOCTORAL

(MENCIÓN INTERNACIONAL)

RIESGO SÍSMICO Y ANÁLISIS DINÁMICO
DE PRESAS ARCO-GRAVEDAD

Doctorando

Enrico Zacchei

Directores

Dr. José Luis Molina González (USAL)

Dr. Reyolando Manoel Lopes Rebello da Fonseca Brasil (USP)

A continuación, se incluirán las autorizaciones de los directores para la presentación de la tesis en el formato de compendio de artículos.

Seguidamente se incluirán, para la obtención de la mención de "doctor internacional", dos informes de dos expertos doctores pertenecientes a instituciones no española y una declaración de la estancia fuera de España.

También se incluirá, para la cotutela, una declaración del codirector de tesis de la universidad extranjera.

Por la presente carta expreso:

1.- Mi aceptación, como coautor de las siguientes publicaciones listadas a continuación, a que el doctorando Enrico Zacchei presente los siguientes artículos como mérito de tesis doctoral.

2.- Declaración de que el doctorando es el autor principal de la investigación recogida en dichas publicaciones.

Publicaciones:

Enrico Zacchei; Molina JL; Reyolando Brasil. Nonlinear Degradation Analysis of Arch-Dam Blocks by using deterministic and Probabilistic Seismic Input. Journal of Vibration Engineering & Technologies. 01/01/2018. ISSN 2321-3558

Enrico Zacchei; Molina JL; Reyolando Brasil. Seismic hazard assessment of arch dams via dynamic modelling: an application to the Rules Dam in Granada, SE Spain. International Journal of Civil Engineering International Journal of Civil Engineering. 13/12/2017. ISSN 1735-0522
DOI: 10.1007/s40999-017-0278-4

Enrico Zacchei; Molina JL; Reyolando Brasil. Seismic Hazard and Structural Analysis of the Concrete Arch Dam (Rules Dam on Guadalfeo River). Procedia Engineering. 2017. ISSN 1877-7058

Ávila, 18 de junio de 2018

ESCOLA POLITÉCNICA DA UNIVERSIDADE DE SÃO PAULO

Avenida Professor Almeida Prado – Travessa 2 – Cidade Universitária - CEP: 05508-900 São Paulo SP
Telefone: (011) 3091-5519 - Fax (011) 3091-5233

_____

Departamento de Engenharia de Estruturas e Geotécnica

TO WHOM IT MAY CONCERN

By this letter I DECLARE:

1.- My acceptance, as co-author of the following publications listed below that compose the Doctoral Thesis of the doctoral candidate Enrico Zacchei.

2.- I declare that the doctoral student is the main author of the research collected in said publications.

Publications:

Enrico Zacchei; Molina JL; Reyolando Brazil. Nonlinear Degradation Analysis of Arch-Dam Blocks by using deterministic and Probabilistic Seismic Input. Journal of Vibration Engineering & Technologies. 01/01/2018. ISSN 2321-3558

Enrico Zacchei; Molina JL; Reyolando Brazil. Seismic hazard assessment of arch dams via dynamic modeling: an application to the Dam Rules in Granada, SE Spain. International Journal of Civil Engineering International Journal of Civil Engineering. 12/13/2017 ISSN 1735-0522 DOI: 10.1007 / s40999-017-0278-4

Enrico Zacchei; Molina JL; Reyolando Brazil. Seismic Hazard and Structural Analysis of the Concrete Arch Dam (Rules Dam on Guadalfeo River). Proceed Engineering. 2017. ISSN 1877-7058

São Paulo, June 18, 2018

Reyolando Manoel Lopes Rebello da Fonseca Brasil
Associate Professor
Department of Structural and Geotechnical Engineering
Polytechnic School, University of São Paulo, Brazil

DIPARTIMENTO DI INGEGNERIA
CIVILE EDILE E AMBIENTALE

SAPIENZA
UNIVERSITÀ DI ROMA

Dr. Giorgio De Donno, **Ph.D.**
Professor of Applied and Environmental Geophysics
Department of Civil, Building and Environmental Engineering
University of Rome "Sapienza"
via Eudossiana, 18 - 00184 Rome Italy
email: giorgio.dedonno@uniroma1.it
tel: +39 06 44 585 076

Rome, 08/06/2018

TO WHOM IT MAY CONCERN

External report on PhD thesis, entitled *"Riesgo sísmico y análisis dinámico de presas arco-gravedad"* by Enrico Zacchei.

The PhD thesis is written as a compendium of three articles published in international peer-reviewed journals, all available in Scopus.

The work focuses on the definition of the seismic input (using both probabilistic and deterministic approaches) and the development and calibration of mathematical models (2D and 3D finite-element and 2D gravity methods) for the dynamic analysis of concrete arch dams, with particular reference to a case study in southern Spain (Rules Dam on Guadalfeo River).

The results reported by papers no. 1 and 2 provided a good agreement between finals mathematical models and observations, highlighting a significant difference between modelled maxima acceleration and those defined by national regulations. Moreover, the application of a non-linear analysis (paper no. 3) shows severe damages as expressed in terms of accumulation of plastic deformation and accumulation of cracks.

Overall, the mathematical and numerical approach is rigorous and innovative, providing new protocols for the analysis and investigation of existent concrete arch dams. The high-quality results are clearly expressed and proved throughout all the three papers.

The PhD thesis represents a high-level innovative work within the scientific community and it can be viewed as the starting point for further studies, which could involve i.e. the comparison between modelling and observations made using non-invasive methods for imaging the dam's structure.

Based on the above arguments, I wholeheartedly recommend the PhD thesis of Enrico Zacchei to the supporting attention of the final Evaluation Committee.

Yours sincerely,

Giorgio De Donno, Ph.D.

Dr. Giorgio De Donno
Ph.D. - Professor of Applied and Environmental Geophysics
University of Rome "Sapienza"
via Eudossiana, 18 - 00184 Rome Italy

TO WHOM IT MAY CONCERN

Dear Sir/Madam,

Analysis of three full papers as a requisite for a PhD thesis:

"Seismic hazard and structural analysis of the concrete arch dam (Rules dam on Guadalfeo River)"; "Seismic hazard assessment of arch dams via dynamic modelling: an application to the Rules dam in Granada, SE Spain"; "Nonlinear degradation analysis of arch-dam blocks by using deterministic and probabilistic seismic input".
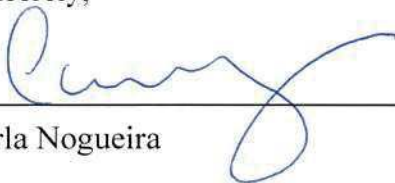
The candidate has performed an interesting work about seismic behaviour of the Rules dam on Guadalfeo River, considering the deterministic and probabilistic approaches for risk and safety assessment. The studies were essentially analytic and numerical and they considered the dam's site information, the proper material parameters as well the real dimensions of the structure, including the fluid-structure interaction.

In the first phase of the study, it was prioritized the modelling of the seismic behaviour of the dam's structure, in which good comparisons with the known information from the literature was obtained. The chosen criterion was the assessment of the stresses on the body's dam to evaluate the potential crack formation in the concrete structure.

The second phase of the study used the obtained information of the dam's seismic behaviour to perform a more realistic structural analysis considering the nonlinear degradation of the concrete stiffness properties. In my opinion, considering what was proposed, it completes the entirely structural analysis of the dam because all the seismic and nonlinear material aspects were taken into account. In an earthquake, the transversal displacements associated to the stresses magnitude may produce plastic hinges along the body's dam, which may contribute to potential damages in time.

The work has high quality and achieves all the PhD standard requirements.

Yours sincerely,

Caio Gorla Nogueira

Professor of the Civil and Environmental Department

Engineering Faculty of São Paulo State University, Brazil

Telephone: +55 (014) 991960024

Email: cgnogueira@feb.unesp.br

FEB
F A C U L D A D E D E
ENGENHARIA BAURU

Faculdade de Engenharia de Bauru
Av. Eng. Luiz Edmundo Carrijo Coube, 14-01 17033-360 Bauru - SP
tel. (14) 3103-6105 sta@feb.unesp.br www.feb.unesp.br

DECLARATION
TO WHOM IT MAY CONCERN

Report on PhD thesis, entitled "Riesgo sísmico y análisis dinámico de presas arco-gravedad" by Enrico Zacchei

The PhD Thesis, written as a compendium of 3 articles published in international peer-reviewed journals, all available in Scopus.

The work is concerned with the necessary seismic deterministic and probabilistic input for the analysis and calibration of mathematical and finite element numerical models for dynamic analysis of concrete arch-gravity dams. The study case is a dam on the Guadalfeo River in Spain.

Papers 1 and 2 report favorable comparisons between the models and observations, with comparisons to the Spanish National Codes on the subject. Non-linear analysis is presented in paper 3 concerning nonlinear material behavior, such as plastification, cracking etc.

The mathematical and numerical work is rigorous and innovative within the scientific community, rendering solid guidelines for the proposed type of structural analysis.

I certify that Mr. Enrico Zacchei, PhD Student, has stayed from May to August, 2018 (4 months) at our Department, as a PhD Student Researcher, coinciding with his doctoral period. During this period, the student carried out research, under my supervision.

São Paulo, June 14th 2018.

Reyolando Manoel Lopes Rebello da Fonseca Brasil
Associate Professor
Department of Structural and Geotechnical Engineering
Polytechnic School, University of São Paulo, Brazil

DECLARATION

Reyolando Manoel Lopes Rebello da Fonseca Brasil, Associate Professor, Department of Structural and Geotechnical Engineering, Polytechnic School, University of São Paulo, Brazil, certifies that Mr. Enrico Zacchei, PhD Student, has stayed from September to November, 2016 (2.5 months) and May to August de 2018 (4 months) at our Department, as a PhD Student Researcher, coinciding with his doctoral period. During this six and a half months, the student carried out research, under my supervision, related to his Thesis subject, seismic hazard and structural analysis of concrete arch dams, via numerical methods..

São Paulo, June 14th 2018.

Reyolando Manoel Lopes Rebello da Fonseca Brasil
Associate Professor
Department of Structural and Geotechnical Engineering
Polytechnic School, University of São Paulo, Brazil

ÍNDICE

FORMATO Y ESTILO DE TESIS

FORMATO

Tesis doctoral en el formato de compendio de artículos/publicaciones previamente aceptados del programa de doctorado "Geotecnologías aplicadas a la construcción, energía e industria", regulado por el R.D. 99/2011. La línea de investigación es: modelización matemática.

NOMBRE Y AFILIACIÓN AUTORES

Los nombres y la afiliación de los autores de los artículos son: Enrico Zacchei, doctorando en la Escuela Politécnica Superior de Ávila, Universidad de Salamanca (USAL), España; José Luis Molina González, Profesor Titular de Universidad de la Escuela Politécnica Superior de Ávila, Universidad de Salamanca (USAL), España; Reyolando Manoel Lopes Rebello da Fonseca Brasil, Profesor Catedrático de Universidad de la Escuela Politécnica de São Paulo, Universidad de São Paulo (USP), Brasil.

REFERENCIA DE LAS REVISTAS Y EL DOI DE LOS ARTÍCULOS

Esta tesis doctoral está compuesta por tres artículos de investigación en prestigiosas revistas científicas internacionales de impacto. Ellas son sujetas a evaluación crítica mediante revisiones anónimas, por pares expertos internacionales y de reconocida trayectoria. Las revistas son:

1.   Procedia Engineering (ISSN: 1877-7058; Elsevier). Revista indexada en Scopus desde 2009 ("cite score" de 2016: 0.74) con énfasis en disciplinas básicas de ingeniería, como ingeniería aeroespacial, química, civil, mecánica o estructural. El artículo científico titulado "Seismic Hazard and Structural Analysis of the Concrete Arch Dam (Rules Dam on Guadalfeo River)", se publicó en septiembre de 2017 (doi: https://doi.org/10.1016/j.proeng.2017.09.334).

2.   International Journal of Civil Engineering (ISSN: 1735-0522; Springer). Revista indexada en Web of Science desde 2010 ("impact factor" de 2016: 0.624) con énfasis en estructuras, geotecnia, transporte, ambiente, terremotos, recursos hídricos, estructuras hidráulicas e hidráulicas, gestión de la construcción y materiales. El artículo científico titulado "Seismic Hazard Assessment of Arch Dams via Dynamic

Modelling: an Application to the Rules Dam in Granada, SE Spain", se publicó en diciembre de 2017 (doi: https://doi.org/10.1007/s40999-017-0278-4).

3.   Journal of Vibration Engineering & Technologies (ISSN: 2321-3558; Krishtel eMaging Solutions). Revista indexada en Web of Science desde 2014 ("impact factor" de 2017: 0.615) con énfasis en ingeniería de vibración e ingeniería mecánica. El artículo científico titulado "Nonlinear Degradation Analysis of Arch-Dam Blocks by using Deterministic and Probabilistic Seismic Input", se publicará en febrero de 2020.

INTRODUCCIÓN

En la literatura hay bastantes artículos publicados sobre la peligrosidad sísmica de las presas en España y, en general en el mundo, hay bastantes artículos sobre este tema[1,2]. No obstante, son pocos los trabajos que aplican el análisis propuesto en esta Tesis Doctoral a una presa arco-gravedad en España. La modelización matemática aquí propuesta será de especial interés a la ingeniería de presas y embalses.

El impacto de las presas en las sociedades es significativo. Su construcción implica el desplazamiento de muchas personas, la pérdida de yacimientos arqueológicos y un cambio ecológico importante. Por tanto, el impacto de la construcción de presas a las poblaciones afectadas y la estricta protección del medioambiente hace que sea imprescindible una modelización precisa de la infraestructura para un diseño óptimo y para conseguir una buena conservación en el tiempo.

Todo esto sin considerar los daños enormes que una presa crea cuando se rompe; generalmente por defectos de construcción, mantenimiento deficiente e insuficiencia de conocimiento técnico. Dos casos históricos emblemáticos son la presa de materiales sueltos de South Fork en los Estado Unidos en 1889, donde murieron 3000 personas y 35000 personas se quedaron sin casa, que se rompió por abandono y por una mala modificación de la estructura solo por conveniencia; y la presa bóveda de Malpasset en Francia en 1959 que a causa de uno desplazamiento de la roca de fundación se rompió y destruyó toda la ciudad aguas abajo[3,4].

Las grandes presas fueron las primeras estructuras diseñadas contra los terremotos en casi todas las partes del mundo desde la década de 1930. Sin embargo, en 1930 el peligro sísmico estaba definido por un coeficiente sísmico de 0.1, totalmente independientemente del contexto sísmico en los sitios de las presas, que a menudo no se conocía, y para el análisis sísmico se utilizaba el método pseudo-estático. Este concepto de análisis fue abandonado en

---

[1]García-Mayordomo, J., Insua-Arévalo, J. M., Seismic hazard assessment for the Itoiz Dam site (Western Pyrenees, Spain), Soil Dynamics and Earthquake Engineering, 31:1051–1063, 2011.

[2]Furgani, L., Verifiche Sismiche di Dighe in Calcestruzzo, Tesis Doctoral, Universidad Roma Tre, Italia, p. 350, 2014.

[3]Levy, M., Salvadori, M., Perché gli Edifici Stanno in Piedi, Ed. Bompiani, Milano, Italia.

[4]Levy, M., Salvadori, M., Perché gli Edifici Cadono, Ed. Bompiani, Milano, Italia.

1989 cuando ICOLD[5] publicó su moderna guía para la selección de parámetros sísmicos para grandes presas, que se actualizó en 2016.

Hoy en día, el método de análisis pseudo-estático y la representación del peligro sísmico por un coeficiente sísmico se consideran obsoletos o incluso incorrecto y, por lo tanto, ya no se utiliza más. Debido a este cambio, probablemente muchas presas, que habían sido diseñadas contra los terremotos con el método pseudo-estático, cumplen los criterios de seguridad sísmica de hoy. Las presas bien diseñadas y bien construidas generalmente son seguras, pero otras pueden ser deficientes, especialmente aquellas ubicadas en áreas de sismicidad moderada-alta.

Las presas que se descuidan tienen una vida útil sorprendentemente corta, mientras las presas bien mantenidas pueden estar en funcionamiento durante más de 100 años.

OBJETO DE ESTUDIO

El caso de estudio es la gran presa de Rules. Esta es una estructura hidráulica arco-gravedad con planta curva que está situada en el rio Guadalfeo, en la provincia de Granada, en la región de la Andalucía (sur de España), entre los municipios de Velez de Benaudalla y Salobreña. El uso de la presa es de abastecimiento, defensa frente a avenida y riego. La obra se finalizó en el año 2003.

El área de estudio es la provincia de Granada que en relación con el mapa de peligrosidad sísmica de la norma española en vigor (NCSE-02[7] y NCSP-07[8]) es un área con alta sismicidad, es decir que es un área de categoría A.

España es considerada como un país de actividad sísmica moderada en consideración a la sismicidad registrada en su catálogo sísmico y de actividad sísmica frecuente como los de otros países del área mediterránea como Italia y Grecia. La situación de la Península Ibérica en el borde de las placas entre África y Eurasia es la que determina la existencia de zonas sísmicamente activas. Al oeste de Gibraltar se encuentra la falla de Azores-Gibraltar. La región

---

[5]International Commission on Large Dams Guidelines (ICOLD), Selecting Seismic Parameters for Large Dams, Bulletin No. 148, 2016.

[7]Comisión Permanente de Normas Sismorresistentes, Norma de construcción sismorresistente: Parte general y edificación, NCSE-02, 2002.

[8]Comisión Permanente de Normas Sismorresistentes, Norma de construcción sismorresistente: Puentes, NCSP-07, 2007.

más activa sísmicamente está limitada al norte por el accidente Cádiz-Alicante y al sur por el norte de Marruecos[9,10,11].

HIPÓTESIS DE TRABAJO

El doble enfoque sismo-estructura que esta tesis aborda ha implicado la necesidad de considerar componentes de estudio diferenciadas. Por tanto, las hipótesis a nivel sísmico y estructural serán divididas.

HIPÓTESIS A NIVEL SÍSMICO

La zona sismogénica donde la presa de Rules está situada es la Cuenca de Granada (ZS35, ZESIS[12]) en la Cordillera Bética. La tectónica dominante es de tipo fallas normales. Aquí se han sucedido terremotos, hasta el 2018, cuya magnitud máxima media ha alcanzado valores de 6.8 con una peligrosidad relativa muy alta. El evento máximo fue de magnitud momento 6.5±0.3 el 25/12/1884. Estos valores de magnitud pueden causar importantes daños a las estructuras.

En la región de Andalucía se suceden continuamente terremotos de magnitud más pequeña que llegan a magnitud 5.2±0.3 y ellos pueden producir también daños notables.

El análisis de la peligrosidad sísmica es hecho con los métodos tradicionales, pero utilizando dados recientes ofrecidos por la base de datos de zonas sismogénicas de la Península Ibérica (ZESIS).

El método probabilístico (PSHA: "probabilistic seismic hazard assessment") y determinista (DSHA: "deterministic seismic hazard assessment") para calcular el riesgo

---

[9]Sanz de Galdeano, C., Peláez Montilla, J. A., López Casado, C., Seismic potential of the main active faults in the Granada basin (Southern Spain), Pure an Applied Geophysics, 160:1537–1556, 2003.

[10]Gaspar-Escribano, J. M., Navarro, M., Benito, B., García-Jerez, A., Vidal, F., From regional to local-scale seismic hazard assessment: examples from Southern Spain, Bulletin of Earthquake Engineering, 8:1547–1567, 2010.

[11]Benito, M. B., Navarro, M., Vidal, F., Gaspar-Escribano, J. M., García-Rodríguez, M. J., Martínez-Solares, J. M., A new seismic hazard assessment in the region of Andalusia (Southern Spain), Bulletin of Earthquake Engineering, 8:739–766, 2010.

[12]IGME (2015) ZESIS: Base de datos de zonas sismogénicas de la Península Ibérica y territorios de influencia para el cálculo de la peligrosidad sísmica en España. http://info.igme.es/zesis

sísmico de la zona de estudio son métodos encontrados en ICOLD y en la literatura[13,14]. Siendo un proceso estocástico hay muchas incertidumbres[15].

HIPÓTESIS A NIVEL ESTRUCTURAL

La presa arco-gravedad de Rules tiene una altura máxima sobre cimientos de 130.0 m, una altura sobre cauce de 100.0 m, una longitud de coronación de 620.0 m, un radio de 500.0 m y una base máxima aproximadamente de 100.0 m. El volumen del cuerpo de la presa es de 2032.0×10^3 m^3. Los taludes de aguas arriba y abajo son de 1:0.18 y 1:0.60, respectivamente.

Los dados hidrológicos de la cuenca son los siguientes: la superficie de la cuenca es de 1070.0 Km^2 con una aportación media anual de 150.0 hm^3 y con una precipitación media anual de 650.0 mm. La capacidad del aliviadero (único aliviadero) es de 2987.0 m^3/s mientras la capacidad del embalse es de 113.0 hm^3. La superficie del embalse a NMN (Nivel Máximo Normal) es de 309.0 Ha y la cota del NMN es de 240.0 m. La avenida de proyecto es de 3020.0 m^3/s. La presa tiene dos desagües de capacidad cada uno entre 79.0 y 187.0 m^3/s. Los dados son tomados en el Inventario de Presas y Embalses del Ministerio de Agricultura y Pesca, Alimentación y Medio Ambiente del Gobierno de España (SNCZI)[16], y en la Sociedad Española de Presas y Embalses (SEPREM)[17].

La modelización matemática del sistema es compuesta de una presa de hormigón, de un embalse de agua, de una fundación y sedimentos. El sistema es un sistema a cuatro componentes. En el análisis todos los cuatro componentes fueron estudiados juntos para obtener resultados más realísticos. Sin embargo, los componentes pueden ser analizados separadamente para mantener un control de los esfuerzos que actúan, pero necesita tener en cuenta que una componente puede afectar las otras aumentando o disminuyendo los esfuerzos.

---

[13]Faccioli, E., Paolucci, R., Elementi di Sismologia Applicata all'Ingegneria, Ed. Pitagora, Bologna, Italy, p. 268, 2005.

[14]Kramer, S. L., Geotechnical Earthquake Engineering, Ed. Prentice-Hall, Upper Saddle River, New Jersey, p. 672, 1996.

[15]Gaspar-Escribano, J. M., Rivas-Medina, A., Parra, H., Cabañas, L., Benito, B., Ruiz Barajas, S., Martínez Solares, J. M., Uncertainty assessment for the seismic hazard map of Spain, Engineering Geology, 199:62–73, 2015.

[16]Inventario de Presas y Embalses (SNCZI), Ministerio de Agricultura y Pesca, Alimentación y Medio Ambiente, Gobierno de España. http://sig.mapama.es/snczi/visor.html

[17]Sociedad Española de Presas y Embalses (SEPREM). http://www.seprem.es/index.php

Una comparación con las normas[18,19] y los métodos clásicos[20,21] para disminuir el margen de error que hay en una modelización fue hecho.

OBJETIVOS

- Estudiar y actualizar el área donde se localiza la presa usando las nuevas zonas sismogénicas del 2015 (ZESIS).

- Obtener los parámetros necesarios para hacer el análisis de la peligrosidad sísmica.

- Modelizar matemáticamente la presa para calcular la estabilidad, estimar el daño de la estructura, el desplazamiento limite, la influencia de la interacción con el embalse y la fundación (cimentación), y las tensiones limite.

- Investigar y desarrollar métodos con rigor académico[22] para el estudio de presas, que es un tema complejo y demandante.

- Rehacer nuevos cálculos de presas nuevas y existentes.

- Estimular los propietarios de las presas a extender la vida económica de sus presas. Esto incluye reanalizar la estructura con nuevos datos sobre terremotos, inundaciones u otros riesgos y revisiones periódicas de seguridad para un mantenimiento adecuado.

---

[18]Consiglio Superiore dei lavori pubblici, Norme Tecniche per la Progettazione e la Costruzione degli Sbarramenti di Ritenuta (Dighe e Traverse), 2009.

[19]European Committee for Standardization, Eurocode 8: Design of structures for earthquake resistance - Part 1: General rules, seismic actions and rules for buildings, EN 1998-1:2004, 2004.

[20]Chakrabarti, P., Chopra, A. K., Earthquake analysis of gravity dams including hydrodynamic interaction, Earthquake Engineering and Structural Dynamics 2:143–160, 1973.

[21]Fenves, G., Chopra, A. K., Effects of reservoir bottom absorption on earthquake response of concrete gravity dams, Earthquake Engineering and Structural Dynamics 11:809–829, 1983.

[22]Eco, U., Come si Scrive una Tesi di Laurea, Ed. Bompiani, Milano, Italia.

PRINCIPALES CONCLUSIONES

- En España hay aproximadamente en total 1200 presas y una importante fracción de éstas se localiza en zonas de sismicidad moderada o alta. La gran mayoría de estas presas fueron construidas antes a las normas sismorresistente española modernas (NCSE-02 y NCSP-07), por tanto, es recomendable reevaluar la peligrosidad sísmica de las presas existentes, particularmente aquellas de categoría A en zonas de sismicidad alta.

- Se ha obtenido una buena calibración entre las observaciones de la estructura y de los dados de "input" sísmico y los resultados finales de la modelización matemática.

- Los resultados del análisis de peligro sísmico han mostrado que las aceleraciones máximas son mucho más altas que los valores definidos en la norma española (NCSE-02 y NCSP-07), que es muy deficiente en estos aspectos.

- En el análisis estático y dinámico lineal y non lineal, los esfuerzos de la presa han excedido la tensión máxima permitida, creando una cantidad de rótulas plásticas. Una presa debe ser cuidadosamente diseñada y mantenida para evitar daños importantes.

RESUMEN DE LOS ARTÍCULOS: METODOLOGÍAS Y RESULTADOS

RESUMEN ARTÍCULO 1

El objetivo de este trabajo es analizar el comportamiento de la presa de Rules a través del cálculo del peligro sísmico desarrollado en la localización geográfica donde está situada la presa. Si quiere también analizar algunos puntos críticos de la presa, así como la interacción fluido-estructura.

Para la metodología del análisis del peligro sísmico véase el resumen del artículo 2.

La presa arco-gravedad debe ser modelada en 2D y 3D de acuerdo con el método teórico clásico[23,24], teniendo en cuenta sus grandes dimensiones. Una presa arco-gravedad debe ser modelada en 3D para considerar la interacción entre los "cantilevers" y "arches". La curvatura del arco aumenta la rigidez de la estructura, por tanto el hecho de no considerar el comportamiento longitudinal es muy simplista. Por otro lado, el comportamiento trasversal se analiza en 2D. La modelización matemática fue hecha usando diferentes programas de cálculos como el SAP2000[25] para una modelización con el Método de Elementos Finitos (MEF) y el CADAM[26] para una modelización con el método de gravedad.

La ley constitutiva del hormigón utilizada para los modelos 2D y 3D es la relación tensión-deformación no lineal definida en el Eurocode[27]. Las características del hormigón de la presa de Rules son: resistencia a la compresión del hormigón = 50 MPa; deformación a la tensión de pico = 2.45‰; módulo de elasticidad = 37 GPa; módulo de elasticidad dinámico = 1.2 x 37 = 44.4 GPa; resistencia de cálculo en tracción = 1547 kN/m² (para hormigón con cemento 50); resistencia de cálculo en tracción = 960 kN/m² (para hormigón con cemento 25).

[23]U.S. Army Corps of Engineers (USACE), Theoretical Manual for Analysis of Arch Dams, Technical Report ITL-93-1, USA, p. 109, 1993.

[24]U.S. Army Corps of Engineers (USACE), Arch Dam Design, Manual No. 1110-2-2201, USA, p. 240, 1994.

[25]SAP2000 (Version 16.0.0 Plus), California/New York: Computers and Structures, Inc.

[26]Leclerc, M., Léger, P., Tinawi, R., CADAM (Version 1.4.14), Montréal, Canada: CRSNG/Hydro-Québec/Alcan, 2004.

[27]European Committee for Standardization, Eurocode 2: Design of concrete structures - Part 1-1: General rules and rules for buildings, EN 1992-1-1:2004, 2004.

En el modelo 3D del SAP2000 el peso específico del hormigón es 24 kN/m^3. Considerando las galerías y las válvulas en el cuerpo de la presa, este valor fue disminuido el 14% (peso específico utilizado = 24 x 0.86 = 20,64 kN/m^3). Esta diferencia se obtuvo a partir de la relación entre el peso real y el peso del modelo: 36368.5 MN/42120.74 MN = 0.86. En el modelo 2D del CADAM y del SAP2000 el peso específico del hormigón es 24 kN/m^3.

La discretización del modelo 3D con el SAP2000 es: radio = 500 m; longitud de coronación = 620 m; ancho de la coronación = 10 m; altura del bloque más alto = 130.33 m; altura del bloque más bajo = 7.0 m; base del bloque mayor = 101.657 m; base del bloque menor = 5.460 m; ángulo de la curvatura en plan de la presa = 71.04°; talud aguas abajo = 1:0.60; talud aguas arriba = 1:0.18; números de elementos sólidos (3.00 x 2.50 x 19.375 m) usadas para el MEF = 32980; números de juntas usadas para el MEF = 36925.

La discretización del modelo 2D con el SAP2000, considerando la sección del bloque central como un triángulo, es: altura = 120 m; base = 93.6 m; ancho de la coronación = 10 m; talud aguas abajo = 1:0.60; talud aguas arriba = 1:0.18; números de elementos sólidos (3.01 x 2.79 x 1.0 m) usadas para el MEF = 683; números de juntas usadas para el MEF = 765.

La discretización del modelo 2D con el CADAM, considerando la sección del bloque central como un triángulo, es: altura = 120 m; base = 93.6 m; ancho de la coronación = 10 m; talud aguas abajo = 1:0.60; talud aguas arriba = 1:0.18; números de bloques horizontales con una altura de 2.5 m cada uno = 48.

Los vínculos de la base en el modelo 2D y 3D del SAP2000 son fijos en todas las tres direcciones en virtud de una fundación rocosa (velocidad de propagación de las ondas elásticas transversales > 750 m/s).

El orden de la magnitud de la rigidez de la base rocosa es de 1 x 10^9 kN/m. La base se vuelve deformable con una rigidez de 1 x 10^6 kN/m. Usando este último valor de rigidez, la tensión vertical debida al peso de la presa proprio de la presa aumenta de 1.476 veces.

En el modelo 2D del CADAM no se tiene en cuenta la interacción entre presa y fundación. Los parámetros de la fundación son: módulo de elasticidad = 41.55 GPa; módulo de Poisson = 0.33; peso específico = 27.47 kN/m^3.

Las cargas aplicadas en el modelo 2D y 3D del SAP2000 son: peso proprio, carga hidrostática e hidrodinámica. Las cargas aplicadas en el modelo 2D del CADAM son: peso proprio, efecto sísmico, sub-presión, carga hidrostática y carga hidrodinámica.

Los resultados son que, en la norma española (NCSE-02 y NCSP-07), la aceleración máxima del terreno es de 0.17 g, mientras en el análisis de este trabajo la mayor aceleración probabilista del suelo es de 0.35 g, que es aproximadamente el doble. Los análisis muestran que las tensiones superan la tracción máxima permitida creando rótulas plásticas. En un análisis determinista la mayor aceleración utilizando el terremoto "España, 1910" es de 1.19 g.

Una presa es una estructura estratégica que debe ser cuidadosamente diseñada para evitar la contaminación del depósito de agua, el daño ambiental de las instalaciones cercanas y para proteger la seguridad humana.

RESUMEN ARTÍCULO 2

Este trabajo tiene como objetivo estudiar de manera completa el peligro sísmico a través del método probabilístico (PSHA) y determinístico (DSHA). El primero obtiene la ocurrencia más probable de terremotos y define el terremoto de proyecto, mientras el segundo obtiene los terremotos más intensos y define el terremoto extremo.

La metodología de la modelización matemática está descrita en el resumen del artículo 1.

El PSHA se calcula utilizando el método de Cornell[28] y se desarrolla en cuatro pasos: (i) identificación y caracterización de las fuentes sismogénicas (ZESIS); (ii) caracterización de las distribuciones de magnitud-recurrencia con la hipótesis de Poisson[29] y ley de Gutenberg y Richter[30]; (iii) evaluación de la aceleración del terreno usando las ecuaciones de atenuación

---

[28]Cornell, C. A., Engineering seismic risk analysis, Bulletin of the Seismological Society of America, 58:1583–1606, 1968.

[29]Ross, S. M., Probabilità e Statistica per l'Ingegneria e le Scienze, Ed. Apogeo, Italy, 2008.

[30]Gutenberg, B., Richter, C. F., Frequency of earthquakes in California, Bulletin of the Seismological Society of America, 34:185–188, 1944.

(Am96[31], Am05[32], BT03[33], SP96[34]); y (iv) cálculo de las curvas del riesgo sísmico. El PSHA fue desarrollado utilizando el programa Crisis[35].

El DSHA se desarrolla en tres pasos: (i) selección del terremoto histórico; (ii) evaluación de la aceleración del terreno usando las ecuaciones de atenuación; y (iii) cálculo de las aceleraciones del espectro sísmico.

Varios acelerogramas se han elegido, desde la base de datos ESM[36], para identificar un terremoto real para hacer un análisis dinámico "time-history" coherente. Los terremotos elegidos fueron elaborados utilizando el programa Seismosignal[37].

El input sísmico del terremoto extremo ha mostrado que las aceleraciones máximas son tres veces más altas que el valor de la norma española (NCSE-02 y NCSP-07). En consecuencia, el estrés ha excedido la tensión máxima permitida, creando una cantidad de rótulas plásticas.

RESUMEN ARTÍCULO 3

Este trabajo tiene como objetivo definir la respuesta dinámico no lineal de los bloques de la presa de Rules.

Para la metodología del análisis del peligro sísmico véase el resumen del artículo 2, mientras para la metodología de la modelización matemática véase el resumen del artículo 1.

---

[31]Ambraseys, N. N., Simpson, K. A., Bommer, J. J., Prediction of horizontal response spectra in Europe, Earthquake Engineering and Structural Dynamics, 25:371–400, 1996.

[32]Ambraseys, N. N., Douglas, J., Sarma, S. K., Smit, P. M., Equations for the estimation of strong ground motions from shallow crustal earthquakes using data from Europe and the Middle East: Horizontal peak ground acceleration and spectral acceleration, Bulletin of Earthquake Engineering, 3:1–53, 2005.

[33]Berge-Thierry, C., Cotton, F., Scotti, O., Griot-Pommera, D. A., Fukushima, Y., New empirical response spectral attenuation laws for moderate European earthquakes, Journal of Earthquake Engineering, **7**:193–222, 2003.

[34]Sabetta, F., Pugliese, A., Estimation of response spectra and simulation of nonstationary earthquake ground motions, Bulletin of the Seismological Society of America, 86:337–352, 1996.

[35]Ordaz, M., Aguilar, A., Arboleda, J., Crisis (Version 5.4), Coyoacán, México: Unam, 2007.

[36]Luzi, L., Puglia, R., Russo, E., ORFEUS WG5, Engineering Strong Motion database (ESM) (version 1.0), Istituto Nazionale di Geofisica e Vulcanologia, Observatories and Research Facilities for European Seismology, 2016.

[37]Seismosignal (Version 4.0.0), Pavia, Italy: Seismosoft Ltd.

La teoría "plastic-degradation" se ha utilizado para definir la reducción del módulo elásto-plástico durante los ciclos de histéresis. Los parámetros que se utilizan para aplicar esta teoría se obtienen mediante literatura y análisis numérico.

La respuesta de los bloques de la presa de Rules bajo cuatro terremotos se ha realizado mediante el uso de una integración directa paso a paso.

El módulo no lineal definido en literatura[38] vale: $E_{d,ei}(1 - d_t)$, donde d_t es el factor de daño a tracción y varía desde 0 (material elástico no dañado) a 1 (material completamente dañado), y $E_{d,ei}$ es el módulo de elasticidad inicial. Usando esta ecuación calculamos la rigidez plástica para cuatro ciclos histeréticos: $\{E_{d,ei}|\ i = 1, 2, 3, 4\}$. El cálculo es analítico.

El término no lineal es, además de la rigidez, la masa. La masa dinámica se ha asumido como el 90% de la masa estática porque (i) 10.0 m de la presa son fijado en la fundación y (ii) la masa modal de participación de los primeros tres modos en las tres direcciones es del 83,7%.

Se han obtenido los desplazamientos no lineales integrando la ecuación de movimiento de un oscilador simple[39,40]. El desplazamiento de la cresta de los bloques de la presa tiene un orden de magnitud de 5.0 a 30.0 cm. Debido a la grande rigidez de la presa, el período estructural es del orden de 0.2 – 0.40 s.

---

[38]Lubliner, J., Oliver, J., Oller, S., Oñate, E., A plastic-damage model for concrete, International Journal of Solids and Structures, 25:299–326, 1989.

[39]Brasil, R. M., Silva, M. A., Introdução à Dinâmica das Estruturas para a Engenharia Civil, Ed. Edgard Blücher Ltda, São Paulo, p. 270, 2013.

[40]Clough, R. W., Penzien, J., Dynamics of Structures, Ed. McGraw-Hill, New York, p. 752, 2003.

APÉNDICE (ARTÍCULOS)

ARTÍCULO 1

X International Conference on Structural Dynamics, EURODYN 2017

Seismic Hazard and Structural Analysis of the Concrete Arch Dam (Rules Dam on Guadalfeo River)

Enrico Zacchei[a,]*, José Luis Molina[b], Reyolando M.L.R.F. Brasil[c]

[a]Ph.D. Student, Higher Polytechnic School of Avila (USAL), 50 Hornos Caleros Street, Zip-Code: 05003, Spain
[b]Associate Professor, Higher Polytechnic School of Avila (USAL), 50 Hornos Caleros Street, Zip-Code: 05003, Spain
[c]Full Professor, Polytechnic School of São Paulo (USP), 380 Prof. Luciano Gualberto Avenue, Zip-Code: 05508-010, Brazil

Abstract

The aim of this paper is to describe the seismic hazard performance on the site of Rules Dam, in Granada province (southern Spain), and the seismic influence on this body's dam, as well as on its critical elements, the reservoir and the interaction fluid-structure. The seismic hazard defines the Deterministic Seismic Hazard Assessment (DSHA) and the Probabilistic Seismic Hazard Assessment (PSHA), which are important to calculate the Safety Evaluation Earthquake (SEE) and the Operating Basis Earthquake (OBE), respectively. This recent seismogenic zone provides important data to do the analysis, such as regional geologic setting, seismic history and seismology. In the Spanish code the Peak Ground Acceleration (PGA) for this area is 0.17 g, however in the current analysis the greatest soil acceleration registered is 0.35 g, which is about twice the value. Three accelerograms (controlling earthquakes), by using the Engineering Strong-Motion database, have been chosen to identify the seism's main characteristics. The dam analysis using different software needs to be done to calculate the vibration periods, the hydrodynamic pressure and the maximal vertical stresses. Time-history analyses have been made to analyze the consequences of a dam failure and to estimate minor damage acceptance. The analyses show that the stresses exceed the tensile maximum allowed creating plastic hinges. There are other factors which can affect the dam's behavior such as the vertical component of the earthquake and the silt in the reservoir bottom. The concrete arch gravity dam needs to be modeled in two- and three-dimensions, in accordance to classic theoretical method and current codes, considering its big dimensions (length of the crest: 620 m; radius: 500 m; area of the reservoir whit a operating level: 308 Ha). A dam is an extremely strategic work which needs to be carefully designed to avoid environmental damage to water reservoirs and nearby facilities and for human security. Given that the recent sources of hazard in Spain are from 2015, it would be advisable to reassess the seismic hazard particularly related to existing dams of category A (Spanish code) in areas of high seismicity.

Keywords: Seismic hazard; concrete arch gravity dam; dynamic analysis.

---

* Corresponding author.
  E-mail address: enricozacchei@usal.es

1. Introduction

The focus of this paper is to describe the seismic risk on Rules dam site and its influence in relation to the interpretation of the fluid-structure's dynamical problems. The seismic hazard of a new seismogenic zone is useful to recalculate the actions on the dam. In particular, deterministic and probabilistic analysis will be made to define the SEE and OBE, respectively, using four different attenuation equations. In the Engineering Strong-Motion database three accelerograms have been chosen to do a time-history analysis and to identify the main characteristics of the controlling earthquakes. The dam is modeled by two- and three-dimensions to account for the interaction of the rock foundation and water. The dam analysis in three dimensions defines the modal analysis and the fundamental dam period (0.284 s). In two dimensions, considering a triangular dam shape, the vertical compressive stresses of the element in the bottom of the upstream face have been calculated. It is useful to do the dynamic analysis to know the cyclic behavior of the material subjected to stresses. During the seism, the water in front of the structure exerts a cyclic dynamic load on the wall and the critical mode occurs during the phase when pressure goes in direction to the wall. This phenomenon added to the inertia dam can reach intense stresses. The study of tensional states is necessary to analyze the consequences of a dam failure and to estimate minor damage acceptance.

2. Seismic hazard of a new seismogenic zone

The seismic hazard assessment has been made on basic criteria, as the Cornell method [10], which is based on (i) earthquake recurrence time following a Poisson process and on (ii) event magnitude that is exponentially distributed by Gutenberg and Richter. The model used includes a total of 11 zones and considers a radius of 150 km from the dam site. The coordinates of the dam are: 36.51° (latitude), - 3.29° (longitude). The mean annual rate of exceedance and the b-values have been taken from the new Spanish seismogenic source model but they have been opportunely recalculated taking in to account the many uncertainties of the procedure [13]. The dam is situated in a rocky stratigraphic profile with an average shear wave velocity over 750 m/s.

2.1. SEE and OBE definition

From the disaggregation analysis – which is made to separate the magnitude and distance contribution that has generated acceleration –, for a dam fundamental period (T_d), the following numbers are obtained: $Mw = 5.9$ (magnitude moment) and $R_{epi.} = 7.5$ km (epicentral distance). In Fig. 1 (right) the Pseudo-Spectra Accelerations (PSA) with these values are shown (T is the structural period). The four attenuation relations do not use the same parameters, therefore the values have been adapted (see [6,7,8,9] for the attenuation relations). In Fig. 1 (left) annual probability of exceedance is shown – expressed in terms of return period – in function of PGA. The differences between the curves depend mainly on attenuation equations used and on their standard deviations: when standard deviation decreases the return period increases. The standard deviation values used range from ± 0.19 to ± 0.29 (for the analytic analysis zero has been used). The green curve values, in Fig. 1 (left), are higher because the equation has not been well-constrained for low magnitudes; therefore the curve overestimates higher T_r. This analysis, through a probabilistic approach, has been made only for the seismogenic zone where the dam is: ZS35 [11].
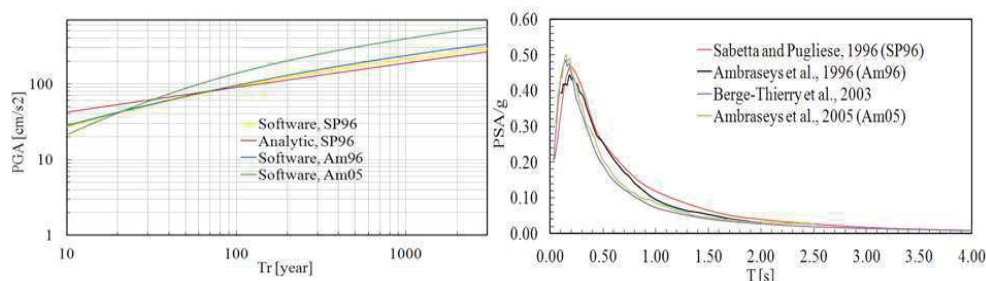

Fig. 1. (left) PGA vs. T_r (used CRISIS2007©software); (right) synthetic spectra.

In Table 1 there are three earthquakes chosen according to disaggregation analysis and the following parameters: M_s (surface-wave magnitude), D_{Ia} (significant duration), R_{jb} (distance from the surface projection of the fault) and the style of fault ruptures that generate the seism. The PGA used in the analysis is 0.25 g. This value is in accordance to literature [16]. The events recorded have been made according to three instrumental orientations (east-west, north-south and up-down) but in Table 1 only the heaviest ones are shown.

Table 1. Characteristic of controlling earthquakes [12] for time-history analyses.

Event, date, time	M_w	M_s	Depth [km]	PGA [cm/s^2]	D_{Ia} [s]	$R_{epi.}$ [km]	R_{jb} [km]	Fault
Greece, 13/09/1986, 17:24:34	5.9	5.7	27.6	234.04	5.17	6.6	-	Normal
Italy, 26/09/1997, 09:40:24	6.0	5.9	5.70	201.39	11.77	4.8	1.63	Normal
Italy, 29/05/2012, 07:00:02	6.0	5.9	8.07	232.12	11.96	9.9	-	Thrust

To design the dam is necessary to calculate the SEE and OBE levels. In the former the damage can be accepted but uncontrolled release of water should not. In the latter these should be none or insignificant damage to the dam. To calculate the SEE the deterministic approach is used; instead, to calculate the OBE the probabilistic approach is used. There are some differences between the two procedures, on important one is that the DSHA does not account for the frequency of earthquake occurrence. In Fig. 2 (left) the Uniform Hazard Spectra (UHS) and controlling earthquakes considering all zones are shown. The UHS provides the accelerations in function of structure period for a fixed return period (in this case: T_r = 1000 years). In Fig. 2 (right) the deterministic spectra obtained for four historical earthquakes by two different attenuation relations are displayed.
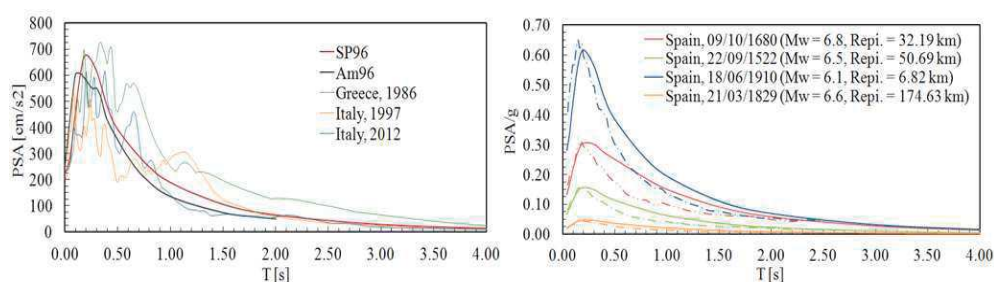

Fig. 2. (left) OBE and controlling earthquakes; (right) SEE by SP96 (in dashed line by Am05).

In the Spanish code [15] the PGA for this area is 0.17 g, however, in the full analysis the soil greatest acceleration registered is 341.72 cm/s^2 which is about twice.

3. Case of study: Rules dam

The Rules dam is situated in southern Spain on the Guadalfeo River in the Granada province. It is an important concrete arch-gravity dam with single curvature in plan, with 620 m of crown length and with radius of 500 m. The maximum height of the vertical cantilever is 130 m and the downstream slope face is 1:0.60. The dam is formed by 32 blocks in total (see Fig. 3). The capacity reservoir for on operating level is 117.07 Hm^3 for a depth (H) of 113 m.

3.1. Direct modeling and analysis

It is necessary to model the arch-dam in two- and three-dimensions because there is an interaction between arch and cantilever units: the load actions create movements that generally consist of three translational and three rotational components. Vertical movements and rotations in vertical tangential planes are considerate negligible [1]. Another important consideration is the interaction between the dam and the rock, in particular, in the abutments where the rock creates a force concentration against the dam. This effect will be not shown in this paper.

Length of the blocks [m]:	No. of the solid elements:	No. of the joints:
19.375	32980	36925
1st dam-reservoir period [s]:	2nd dam period [s]:	3rd dam period [s]:
0.344	0.245	0.208

Fig. 3. (left) Rules dam; (right) dam 3D model and some data – SAP2000©software.

The assumptions adopted to model the dam and to calculate the pressures are in the references [4,5]. Regarding them, it is possible to do some considerations: the upstream face of the dam is not vertical but has inclination of 10,20°, which reduce the horizontal hydrodynamic forces. When water is assumed as compressible, the pressures depend on frequency; in this case, when the natural frequency of the reservoir is close to the natural frequency of the dam-reservoir system, the $P_{hyd, compressible}$ (see Table 2) is 80.72 times greater. Considering the damping, the result is similar, as the range of the damped dam, reservoir and foundation is not large: 2.0 % - 8.5 %. In Table 2 the $P_{hyd, incompressible}$ are also shown (C_w tends to infinity). The numerical simulation has been made by Finite Element Method (FEM) and the gravity method. The FEM has been used for two- and three-dimensions; instead, the gravity method has been used only for 2D analysis. The last method is based on rigid body equilibrium and on beam theory. In the FEM analysis the solid elements have a dimension of 3.00 m per 2.50 m to account for the monolith joints in accordance to literature [2]. The solid element has eight nodes; each one has three translation degrees. The presence of the monolith joints is fundamental to study the nonlinear effects, which are: concrete cracking (the crack opens and closes during the earthquake), water cavitation, temperature, horizontal and vertical construction joints opening during earthquake shaking, formation of plastic hinges, geometrical nonlinearity and sliding on the base [3]. In this example, the input data used are: E_c = 44.40 GPa (modulus of elasticity of the concrete), γ_c = 24 kN/m^3 (mass density of the concrete[1]), ν_c = 0.20 (Poisson's ratio of the concrete), ξ_d = 5.0 % (dam damping), E_f = 41.55 GPa (modulus of elasticity of the foundation rock), γ_f = 27.47 kN/m^3 (mass density of the foundation rock), ν_f = 0.33 (Poisson's ratio of foundation rock), ξ_s = 8.5 % (system damping), T_s = 0.393 s (system fundamental period), γ_w = 10 kN/m^3 (mass density of water), C_w = 1438 m/s (velocity of pressure waves).

3.2. Results: fluid-structure interaction

In Table 2 the hydrodynamic and hydrostatic (P_{hys}) analytical pressures along the height of the dam are shown (the y axis is zero in the bottom of the reservoir). In the fourth column (Relative Error) there are the differences between the hydrodynamic pressures calculated analytically and by CADAM2000©software ($P_{hyd, software}$). The mainly difference depends on the fact that the first pressure is obtained considering a parabolic distribution for a rigid dam while the second pressure take into account the dam deformation, i.e. the acceleration of the dam in the form of vibrations (in this case, the first three modes have been considered). The analytical pressures have been calculated idealizing the dam as a triangular shape because the transversal behavior is similar to a thick gravity dam with a large thickness of the base. The pressures P_{hyd} have been calculated using the wave reflection coefficient α_w = 0.41. It is the ratio of the amplitude of the reflected hydrodynamic pressure wave and the amplitude of a vertical propagating pressure wave incident on the reservoir bottom. This coefficient indicates that the waves are partially reflected in the reservoir and partially transmitted into the substrate. It depends on the impedance, i.e. the dynamic stiffness between the layer of the reservoir and the layer of the rocks. This coefficient identifies the complex interface forces in the frequency domain between both layers. When this coefficient is one (rigid foundation) the pressure has the same values of the analytical $P_{hyd, compressible}$. Another part of the energy is lost due to radiation of pressure waves in the upstream direction. The hydrostatic pressure is affected by the increase or reduction

---

[1]In the 3D analysis, to consider the presence of the galleries and drains in the body's dam, the mass density of the concrete is less than 14 %.

(depending on the acceleration direction) of the effective volumetric weigh of water. According to d'Alembert principle, when the acceleration is directed upwards the hydrostatic pressure decreases. There is a positive effect due to hydrodynamic pressure: in general, arch dams are stiffened by the pre-stress, therefore it is more advantageous to build them instead of constructing gravity dams [17]. The equations used to calculate the hydrodynamic pressure with compressible and incompressible water are in the references [5].

Table 2. Results of the analysis. The upstream pressures are expressed in kN/m^2.

y/H	$P_{hyd, software}$	$P_{hyd, compressible}$	Relative Error	P_{hys}	$P_{hyd, incompressible}$	$^2P_{hyd}$	$^2P_{hyd, vertical}$	P_{hyd}/P_{hys}
0.95	17.15	22.21	1.30	58.36	11.88	25.20	25.45	0.43
0.79	53.50	76.73	1.44	233.38	46.72	99.10	100.54	0.42
0.58	100.91	118.46	1.17	408.41	88.37	187.47	193.18	0.46
0.42	149.07	167.50	1.12	641.79	113.54	240.86	253.07	0.38
0.21	242.10	282.48	1.17	875.16	136.08	288.68	315.11	0.33
0.00	337.79	350.55	1.04	1108.53	143.88	305.22	352.42	0.28

Besides, to determine the sliding, overturning and uplifting of the stability analysis, it is also necessary to calculate the cantilever and the arch stresses. Figure 4 shows the time-history of the stresses (σ_y) of the upstream bottom element of the vertical cantilever of the higher block of the dam (see Fig. 3). Figure 4 shows the case of empty and full reservoirs and both dynamic actions: seismic deadweight (including self-weight) and hydrodynamics. For the empty reservoir the accelerations of the first event (see Table 1) has been used. The "unfavorable" case, obtained through the acceleration of the third event, means that all forces have the same sign. It is possible to see that there is little difference between the analytical and computational analysis.
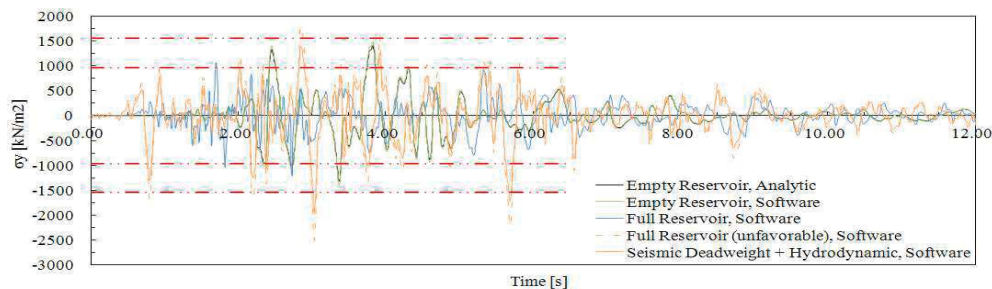

Fig. 4. Time-history of the analytic and computational analysis (Seismosignal©software).

The full reservoir analysis of the second event, by using software, demonstrates that the stresses are lower due to the hydrostatic and uplift negative stresses, but during the seism, uplift pressures within the crack can be assumed to be zero, therefore the σ_y total increases. The stress analysis determines the potential crack and the plastic hinge formation. For each vibration it accumulates plastic deformations producing a hysteretic behavior that depends on dissipated energy. From Eurocode 2 [14] the tensile maximum value adopted that generates significant nonlinear plastic deformations is $f_{ctd} = 1547$ kN/m^2 (dashed red line in Fig. 4). In Fig. 4 other tensile strength of the concrete with lower characteristics ($f_{ctd} = 960$ kN/m^2) is shown – this type of the concrete can be used for gravity dams. When the stress exceeds this value it is necessary the nonlinear analysis to complete the seismic evaluation and to know the capacity of the structure to cumulate the inelastic deformations. This consideration, in the original project of the dam, may have not been made accurately since that the structure was built earlier (in 2003) than the modern seismogenic zone.

---

[2]Hydrodynamic pressure (horizontal and vertical) with effects of reservoir bottom absorption [4].

4. Conclusions and future research

In this paper a complete seismic hazard of the dam site and a dynamic analysis to define the stresses in the body's dam has been made. The first consideration is that, in the Spanish code, the PGA that should be used is 0.17 g; however, for deterministic analysis the value is 0.25 g, i.e. 1.47 greater. Considering all the analyses the value is 2.05 greater. Using these acceleration values, the dynamic analysis has been made to determine the potential crack and the formation of plastic hinges. It is possible to see that for full reservoir (unfavorable) the stress values exceed the tensile maximum value that generates nonlinear deformations. Since that the dam was built in 2003 while the new seismogenic zones were made in 2015, these considerations may not have been taken into account in the original project. Therefore it would be advisable to reassess the seismic hazard, particularly in relation to existing dams of category A (Spanish code) in areas of high seismicity. This paper also aimed to encourage the reduction of the gap between theory research and practical engineering. A dam is a strategic structure which needs to be carefully designed to avoid environmental damage to water reservoirs and to maintain human security, for this the authors will develop other papers about these issues: stochastic dynamic analysis and Bayesian probabilistic method.

Acknowledgements

References

[1] U.S. Army Corps of Engineers (USACE), Theoretical Manual for Analysis of Arch Dams, Technical Report ITL-93-1, Washington, D.C., July 1993, pp. 108.

[2] U.S. Army Corps of Engineers (USACE), Arch Dam Design, Manual No. 1110-2-2201, Washington, D.C., 31 May 1994.

[3] G. Fiorentino, L. Furgani, C. Nuti, F. Sabetta, Seismic Hazard and Use of Strong Motion Time Histories for Dam Seismic Analyses, Second European Conference on Earthquake Engineering and Seismology, Istanbul, August 25-29, 2014.

[4] G. Fenves and A.K. Chopra, Effects of Reservoir Bottom Absorption on Earthquake Response of Concrete Gravity Dams, Earthquake Engineering and Structural Dynamics, Vol. 11, pp. 809-829, 1983.

[5] P. Chakrabarti and A.K. Chopra, Earthquake Analysis of Gravity Dams Including Hydrodynamic Interaction, Earthquake Engineering and Structural Dynamics, Vol. 2, pp. 143-160, 1973.

[6] F. Sabetta and A. Pugliese, Estimation of Response Spectra and Simulation of Nonstationary Earthquake Ground Motions, Bulletin of the Seismological Society of America, Vol. 86, No. 2, pp. 337-352, April 1996.

[7] N.N. Ambraseys, K.A. Simpson and J.J. Bommer, Prediction of Horizontal Response Spectra in Europe, Earthquake Engineering and Structural Dynamics, Vol. 25, pp. 371-400, 1996.

[8] C. Berge-Thierry, F. Cotton and O. Scotti, New Empirical Response Spectral Attenuation Laws for Moderate European Earthquakes, Journal of Earthquake Engineering, Vol. 7, No. 2, pp. 193-222, 2003.

[9] N.N. Ambraseys, J. Douglas, S.K. Sarma, Equations for the Estimation of Strong Ground Motions from Shallow Crustal Earthquakes using Data from Europe and the Middle East: Horizontal Peak Ground Acceleration and Spectral Acceleration, Bulletin of Earthquake Engineering, 3 (1), pp. 1-53, 2005.

[10] C.A. Cornell, Engineering Seismic Risk Analysis, Bulletin of the Seismological Society of America, Vol. 58, No. 5, pp. 1583-1606, October 1968.

[11] IGME (2015) ZESIS: Base de Datos de Zonas Sismogénicas de la Península Ibérica y territorios de influencia para el cálculo de la peligrosidad sísmica en España, http://info.igme.es/zesis.

[12] L. Luzi, R. Puglia, E. Russo & ORFEUS WG5 (2016), Engineering Strong Motion Database, version 1.0, Istituto Nazionale di Geofisica e Vulcanologia, Observatories & Research Facilities for European Seismology, doi: 10.13127/ESM, Accessed on: 16th of December, 2016, Database web site available at: esm.mi.ingv.it.

[13] J.M. Gaspar-Escribano, A. Rivas-Medina, H. Parra, L. Cabañas, B. Benito, S. Ruiz Barajas, J.M. Martínez Solares, Uncertainty Assessment for the Seismic Hazard Map of Spain, Engineering Geology, 199, pp. 62-73, 2015.

[14] European Committee for Standardization (CEN), Eurocode 2: Design of Concrete Structures, Part 1-1: General Rules and Rules for Buildings, EN 1992-1-1:2004.

[15] Comisiòn Permanente de Normas Sismorresistentes, Norma de Construcción Sismorresistente: Parte General y Edificación (NCSR-02), 2002.

[16] J.M. Gaspar-Escribano, M. Navarro, B. Benito, A. García-Jerez, F. Vidal, From Regional- to Local-Scale Seismic Hazard Assessment: Examples from Southern Spain, Bulletin of Earthquake Engineering, 8, pp. 1547-1567, 2010.

[17] T.B. Amina, B. Mohamed, L. André, B. Abdelmalek, Fluid-Structure Interaction of Brezina Arch Dam: 3D Modal Analysis, Engineering Structures, 84, pp. 19-28, 2015.

ARTÍCULO 2

RESEARCH PAPER

CrossMark

Seismic hazard assessment of arch dams via dynamic modelling: an application to the Rules Dam in Granada, SE Spain

Enrico Zacchei[1] · José Luis Molina[1] · Reyolando Manoel Lopes Rebello da Fonseca Brasil[2]

Abstract

Dams are extremely strategic structures that must be carefully designed for human and environmental safety. This paper aims to analyse the influence of probabilistic and deterministic seismic hazards, defined for the site, on the singular points of the Rules dam in southern Spain. A comparison with the data from a recent seismogenic zone (2015) has been made; the adopted criteria for the comparison have been carefully explained. Seismic input from the Safety Evaluation Earthquake has shown that maximum accelerations are three times higher than the Spanish code value. Consequently, the stress has exceeded the maximum allowed tension, creating a number of plastic hinges. To consider the fluid–structure–foundation interaction, 2D and 3D mathematical models have been developed via finite element and gravity methods. A good calibration between the observations and modelling output has been obtained.

Keywords Dynamic analysis · Hydraulic structure · Rules arch-dam · Seismic hazard · Two- and three-dimensional models

Abbreviations

THA	Time-history analysis
PSHA	Probabilistic Seismic Hazard Assessment
DSHA	Deterministic Seismic Hazard Assessment
OBE	Operating basis earthquake
SEE	Safety evaluation earthquake
PSA	Pseudo-spectra acceleration
ZS	Seismogenic zones
IGN	National Geographic Institute
IAG	Andalusian Institute of Geophysics
PDF	Probability density function
PGA	Peak ground acceleration
ESM	Engineering strong-motion
UHS	Uniform hazard spectra
FEA	Finite element analysis

1 Introduction

This paper describes the seismic evaluation of the Rules dam (located in Granada, Spain), a concrete arch-gravity dam, via time-history analysis (THA). Probabilistic Seismic Hazard Assessment (PSHA) and Deterministic Seismic Hazard Assessment (DSHA) have been used to define the seismic data input. The former is necessary to calculate the Operating Basis Earthquake (OBE), which defines any low-level damage to the dam, whether insignificant or absent. The latter is used to calculate the Safety Evaluation Earthquake (SEE), which defines significant levels of damage, such as events resulting from uncontrolled water flow that has not been released, which could lead to catastrophic consequences. The main difference between the probabilistic and deterministic analyses is that the former considers the earthquake frequency, whereas the latter provides a straightforward framework for evaluating the worst possible case of ground motion. The Cornell Method [1] is the procedure that defines the PSHA; it is based on three assumptions: the events are independent and stationary in time; the probability distribution of the magnitude is defined by an exponential distribution, and the seismicity is uniformly

✉ José Luis Molina
  jlmolina@usal.es

  Enrico Zacchei
  enricozacchei@gmail.com

  Reyolando Manoel Lopes Rebello da Fonseca Brasil
  reyolando.brasil@gmail.com

1 Higher Polytechnic School of Ávila, University of Salamanca (USAL), 50 Hornos Caleros Avenue, 05003 Ávila, Spain

2 Polytechnic School of São Paulo, University of São Paulo (USP), 380 Prof. Luciano Gualberto Avenue, 05508-010 São Paulo, Brazil

🌀 Springer

distributed in each seismogenic zone (in contrast to Kernel Method [2], which disregards the seismogenic zones). A DSHA considers the seismic-geological context and the historical earthquake data, which represent different ground motion accelerations. The current data analysis considers the dam location and any uncertainties of the procedure [3]. The probability density function (PDF) and the pseudo-spectra acceleration (PSA) for different return periods have been calculated; the results have been compared to similar results from a previous analysis. Some uncertainties of the PSHA are due to incorrect values from the catalogue. For example, different magnitudes are due to the existence of different types of seismic waves, equations and records. To perform an accurate analysis, the data must be corrected via homogenization, declustering and completeness [4]. These corrections have been explained below.

To evaluate the seismic response of dams, a mathematical model in two and three dimensions has been developed. This model consists of a 3D analysis that considers the block interactions and a 2D analysis that considers vertical and horizontal stresses. The vertical stresses have been calculated using the upstream and downstream faces of the dam wall. To account for the interaction between fluid–structure–foundation observed by the system, geometrical and material parameters have been considered.

The Rules dam was built in 2003, and the new seismogenic zones were created in 2015; as a result, the considerations exposed here may not have been considered in the original project. Many arch dams in the world may face similar problems. Therefore, seismic hazard reassessment is advisable, particularly for existing category A dams [5] in areas of high seismicity. Many important regions of the world are vulnerable to seismic activity; consequently, risk assessments must be made to ensure that vulnerable areas are protected.

2 Seismic risk analysis: explanation of criteria

2.1 Probabilistic seismic hazard analysis

The main characteristic of probabilistic seismic hazard analysis is that it considers earthquake frequency. The basic Cornell method is used in this study; it is based on the Poisson process and Gutenberg–Richter law [6, 7]. In this section, the probabilistic seismic hazard analysis and its chosen criteria will be explained. The new Seismogenic Zones (ZS) of the Iberian Peninsula, established in 2015, are also considered [8]; this map is formed by 55 superficial zones and four deep zones. Earthquakes have the same probability of occurrence at any point inside the zone regardless of its size. This is an important condition when applying the

Cornell method, particularly since additional seismogenic zones exist in previous literature [9]. To start, hazard analysis from the historic catalogue must be examined. In this study, the Instituto Geográfico Nacional (IGN) catalogue has been used [10]. This catalogue contains information about the intensity, magnitude and depth of earthquakes in the Andalusia area. The relative range of the coordinates is $-8°$ to $0°$ (longitude) and $35°$ to $39°$ (latitude). There are other catalogues, e.g., Andalusian Institute of Geophysics (IAG) [11], that can be integrated if the data are incomplete. However, the authors determined that the IGN catalogue data and the number of the used zones are sufficient to carry out this analysis. To perform the probabilistic analysis, four attenuation relations (SP96, Am96, Am05, BT03) [12–15] have been used (see Table 1). The use of these attenuation equations is justified by the fact that they were calibrated using data from Italian records. Note that the Italian tectonic activity is the result of a somewhat similar geological context to that in our area of study [16]. In general, these equations have been largely used in the South-European context.

The homogenization of the magnitude was made to provide the unique moment magnitude (M_w); this is necessary because the data from the IGN catalogue contain five different magnitudes and macro-seismic intensity values. To perform this operation, updated equations and methods from recent literature have been used [17–19]. To use the Poisson process (independence between events), fore-shocks, after-shocks and swarms (in time and space) must be eliminated. The analysis of completeness must be made to correctly estimate the mean annual rate of exceedance (λ_c). This analysis considers the periods that contain an adequate number of seismic events. For example, in the uncorrected catalogue of this analysis, there are only 96 seismic events between 1406 and 1795, whereas in the period between 1796 and 2013, there are more than 16,795 events. If only 96 events were considered in a large period, λ_c would be underestimated. In Fig. 1a, 12,058 uncorrected events within a radius of 150 km from the case study (black point) are shown. To

Table 1 Attenuation equations applied to define the PSA (g)

Abbreviation	Complete definition of attenuation relationships[a]
Am05	$\mathrm{PSA} = 10^{\{a_1 + a_2 M_w + (a_3 + a_4 M_w)\log\sqrt{R_{jb}{}^2 + a_5^2} \pm \sigma\}}$
Am96	$\mathrm{PSA} = 10^{\{C_1' + C_2 M_s + C_4 \log(R_{jb}) \pm \sigma\}}$
SP96	$100 \times \mathrm{PSA} = \omega 10^{\{a + b' M_s + c\log_{10}(R_{epi.}{}^2 + h^2)^{1/2} \pm \sigma\}}$
BT03	$100 \times \mathrm{PSA} = 10^{\{a(f)M_s + b(f)R_{hyp.} - \log_{10}R_{hyp.} + c_1(f) \pm \sigma\}}$

[a]The equations are for the rock sites. The coefficients {a_1, a_2, a_3, a_4, a_5, C_1', C_2, C_4, ω, a, b', c, h, $a(f)$, $b(f)$, $c_1(f)$} of the attenuation relationships can be found in the literature [12–15]. In Am05, the faulting mechanism is not considered. In BT03, $R_{hyp.}$ (km) corresponds to the hypocentral-Rules dam distance. σ is the standard deviation defined in the text
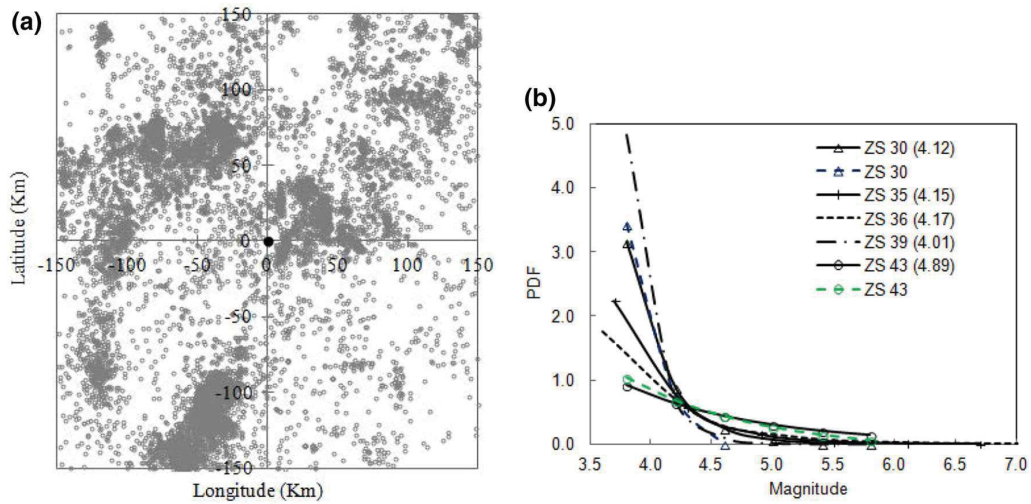
Fig. 1 Earthquakes within a radius of 150 km from the Rules dam (**a**) and probability density function for five seismogenic zones—its mean value is shown in brackets (**b**)

make these operations (catalogue declustering, homogenization and completeness) practical, only the events in the 11 seismogenic zones (Zesis) have been considered. These 11 zones are within a radius of 150 km, which is the recommended distance to adopt the attenuation equations. To eliminate the duplicates, there are some approaches suggested in the literature [20]. Blocks of events with the same latitude and longitude (or with an allowable displacement difference of 0.5 decimal degrees) were considered; later, the largest magnitude events were identified, and any events below this threshold magnitude were eliminated. The maximum reasonable time interval was 90 days. To perform the completeness analysis, the cumulative earthquakes-per-year method has been used. The method uses linear regressions by dividing the magnitude into variance groups, ΔM_w. For both cases (declustering and completeness), a visual method

has been utilized. The Gutenberg and Richter exponential distribution was applied to define a (vertical intercept) and b (slope) parameters (see Table 2). The a-parameter represents the seismic activity; the greater the a-value is (in this analysis the range is 1.36–7.52), the higher the seismicity of the zone. In Table 2, the mean annual rate of exceedance, b-value, β-value, $m_{,max}$ and $m_{,min}$ are shown; λ_c depends on the earthquake's time distribution, completeness time interval and number of reported events. Thus, if λ_c increases, then the number of events increases, or the time interval decreases. The b value describes the relative likelihood of small and large earthquakes. In this analysis, this value ranges between 0.40 and 2.09. When the values have a shallow slope (approximately 0.40–0.97), the small earthquakes have a lower frequency compared to the strong earthquakes in the zone; thus, the seismic hazard is high in this case.

Table 2 Data of the probabilistic analysis

ZS	λ_c	b	β^a	$m_{,max}$	ΔM_w	$m_{,min}$	$\Delta\lambda_c$	Δb	$\Delta m_{,max}$	$\Delta(\Delta M_w)$
29	0.241	0.91	2.08	6.8	0.40	3.6	− 0.05	0.11	− 0.2	0.00
30	0.086	1.37	3.16	4.6	0.20	3.8	− 0.03	− 0.11	0.4	0.20
34	0.296	0.83	1.92	6.7	0.30	3.7	− 0.10	0.17	− 0.1	0.00
35	0.556	0.97	2.24	6.7	0.30	3.7	0.02	0.15	0.1	0.00
36	0.159	0.76	1.75	6.8	0.40	3.6	− 0.02	0.22	− 0.2	0.00
37	0.546	1.10	2.54	5.4	0.20	3.8	− 0.16	0.06	<u>1.4</u>	0.00
38	0.453	0.82	1.88	6.6	0.20	3.8	− 0.14	0.14	0.1	0.00
39	0.113	2.09	4.82	5.0	0.20	3.8	− 0.03	− <u>0.75</u>	<u>1.7</u>	− 0.10
40	0.441	0.93	2.14	6.1	0.30	3.7	− <u>0.31</u>	0.01	0.4	0.00
43	0.659	0.40	0.92	6.2	0.20	3.8	<u>0.23</u>	<u>0.67</u>	0.8	0.00
55	0.667	0.94	2.17	6.8	0.40	3.6	− 0.04	0.09	− 0.1	− 0.10

[a] This value is defined by: $\beta = b \ln 10$

When b is approximately more than 1.00, the seismic hazard is low. The $m_{,max}$ and $m_{,min}$ values are needed to define the PDF and represent its upper and lower limits (see Fig. 1b). The PDF indicates the likelihood that a particular magnitude exceeds a certain $m_{,min}$. For ZS 30 and ZS 43 (dashed line), the PDF also has an upper limit $m_{,max}$. The upper and lower truncated curves likely have small magnitudes, and therefore, the curves are slightly higher. The PDF of ZS 39 is high; it is characterized by events that release energy from small earthquakes. Table 2 shows the values of this study; in the last four columns, the difference (Δ) between the data from this study and the Zesis study (the negative values indicate that the Zesis data are lower than our data) is provided, and some differences can be seen (values are underlined). When considering $\Delta m_{,max}$, the macroseismic intensity changes for a magnitude range of ±0.5, while the physical significance of $\Delta\lambda_c$ and Δb changes to ±0.15 and ±0.35, respectively.

The disaggregation analysis has been performed to separate the magnitude and distance contributions that generated acceleration. The values of the analysis are chosen according to the dam's fundamental period (T_d), return period (T_r) and Peak Ground Acceleration (PGA). The last parameter, obtained by software (Crisis) [21], differs greatly from the design values obtained by PSHA due to wide intervals of T_r. Therefore, the results depend on the first two periods. Three different return periods have been considered: 475-, 1000- and 5000-years; the following values are obtained as a result: M_w = 4.7 and R_{epi} = 7.5 km (epicentral-site distance); M_w = 5.9 and R_{epi} = 7.5 km; M_w = 6.1 and R_{epi} = 7.5 km, respectively. The 1950-year period is a fourth return period that has been considered; it will not be shown in the PSHA since the PSA values are approximately 1.65 more than the values of the 475-year period.

2.2 Deterministic seismic hazard analysis

The deterministic seismic hazard analysis is needed to define the worst earthquake. Since the analysis does not consider the probability of occurrence (return period), it is convenient to consider the standard deviations (σ) of the attenuation equations. The standard deviation values used range from ±0.19 to ±0.26. For a strategic structure, such as a dam, the return period is generally very large. For this reason, the probabilistic analysis alone can be unreliable. A deterministic analysis should be carried out using the seismic-geological context [22] and the historical earthquake data. In Table 3, five controlling earthquakes were chosen according to the disaggregation analysis and the PGA obtained from the PSHA. The earthquake details have been taken from the Engineering Strong-Motion (ESM) database [23], and their analyses have been performed by software (Seismosignal) [24]. The recorded data have considered the three orientations (east–west, north–south and up–down), but only the heaviest results are shown (Table 3). The seismic events are superficial, e.g., the hypo-central distance (depth) is up to 30 km. The other four events are historical earthquakes in Spain.

3 Materials and methods

The mathematical model must be made in two and three dimensions because there is an interaction between arch and cantilever units. The actions create six components—three translational and three rotational (vertical movements and rotations in vertical tangential planes are neglected). The modelling is divided into three parts: 3D analysis considers the arch effects, 2D analysis studies the vertical and

Table 3 Series of records used in the analysis

Location	Date, time	M_w	M_s	Depth (km)	PGA (cm/s²)	R_{epi} (km)
Messinia, Greece	13/09/1986, 17:24:34	5.9	5.8	27.6	234.04	6.625
Foligno, Italy	26/09/1997, 09:40:24	6.0	6.1	5.7	201.39	4.804
Medolla, Italy	29/05/2012, 07:00:02	6.0	5.9[a]	8.07	232.12	14.249
Adra, Spain	16/06/1910, 04:16:41	6.1	6.0[a]	–	–	6.82[a]
Alhama de Almería, Spain	22/09/1522, 10:00:00	6.5	6.5[a]	–	–	50.69[a]
Torrevieja, Spain	21/03/1829, 18:39:00	6.6	6.6[a]	–	–	174.63[a]
Málaga, Spain	09/10/1680, 07:00:00	6.8	6.8[a]	–	–	32.19[a]
Bjeliši, Montenegro	15/04/1979, 06:19:41	6.9	6.9	3.79	356.23	6.841
Pınarlar Köyü, Turkey	12/11/1999, 16:57:19	7.3	7.4	10.4	343.79	5.274

[a] Estimated values (representing an epicentral distance to the Rules dam and the surface-wave magnitude, M_s)

Additional important data are indicated as follows. Significant duration, D_{Ia} (sec): Greece = 5.13; Italy (1997) = 11.77; Italy (2012) = 11.96; Turkey = 10.98; Montenegro = 21.27. Distance between site and the surface projection of the fault, R_{jb} (km): Italy (1997) = 1.63; Italy (2012) = 9.4; Turkey = 8.64; Montenegro = 2.97. Style of fault ruptures that generate the seism: normal faulting in Greece and Italy (1997); thrust faulting in Italy (2012) and Montenegro; strike-slip faulting in Turkey
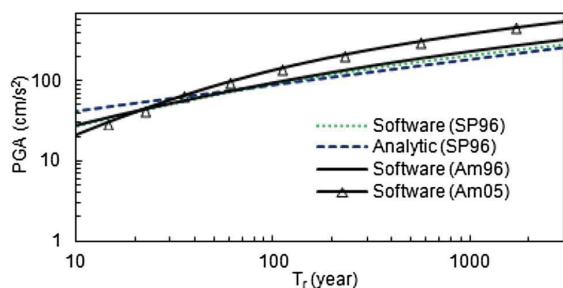
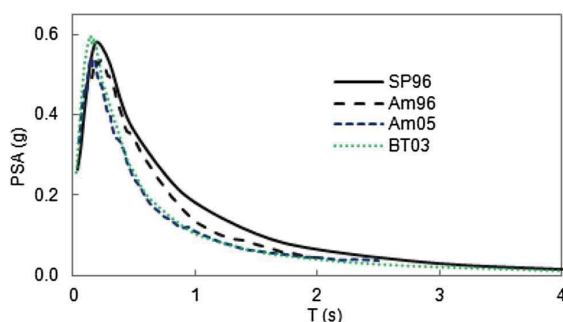**Fig. 2** PGA in function of the return period for the ZS 35 (site of the dam)

Fig. 3 Four synthetic spectra for 1950 years

Fig. 4 Probabilistic spectra using T_r for 475 years and 1000 years, and two controlling earthquakes
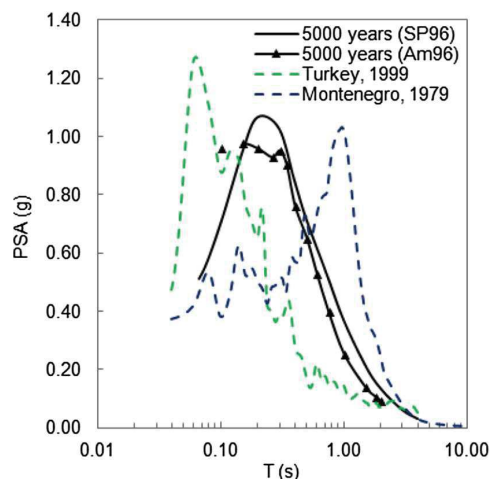
Fig. 5 Probabilistic spectra using T_r for 5000 years and two controlling earthquakes

horizontal stresses, and 2D analysis via the gravity method studies the stability (only some results will be shown). To consider the interactions among liquid, structure and rock observed by the system, geometry and material parameters have been specified. Certain earthquakes have been chosen to perform the THA. The vertical stresses (normal and principal) have been calculated in the upstream and downstream faces of the dam wall; therefore, the exceedance that produced the plastic hinges was estimated.

To design the structure, the SEE and OBE levels were defined and calculated via deterministic and probabilistic approaches, respectively [25]. In Fig. 2, the annual probability of exceedance from Crisis is shown for ZS 35. The differences between the curves mainly depend on the attenuation equations used and on their standard deviations, e.g., if the standard deviation decreases, then the return period increases. The standard deviation values used a range from ± 0.19 to ± 0.29. For the analysis, zero has been used, and the source has been approximated via a circular region with a 47-km radius. The solid-triangle curve points, shown in Fig. 2, are higher because the equation was not well-constrained for low magnitudes; therefore, the curve overestimates the acceleration with a higher T_r. In Fig. 3, the PSAs calculated using values obtained by disaggregation analysis are shown (the pair values, M_w and
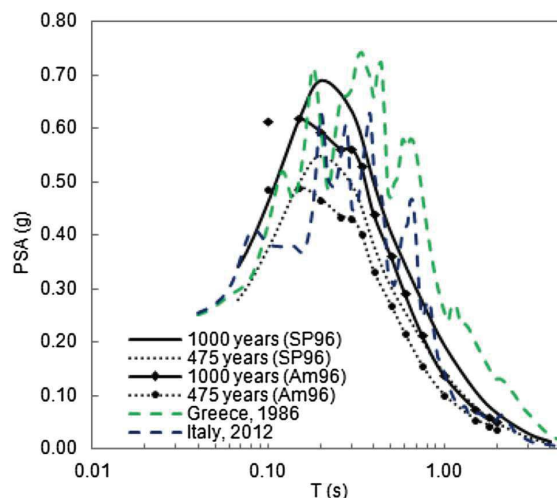
R_{epi}, used are the same for the 5000-year period). Because of the limited interaction of the software, the curves refer exactly to the following return periods: 455-, 1023-, 1949- and 4835-years. This difference is irrelevant for the analysis of the output data. The attenuation equations do not use the same magnitude and distances; therefore, the values are estimated. The distances, shown in Fig. 3, are as follows: 5.5 km for Am96 and 10 km for BT03. The Uniform Hazard Spectra (UHS), which considered all the zones and four controlling earthquakes, are shown in Figs. 4 and 5. The UHS provides the accelerations, which depend on the structure periods (T) for a fixed return period. The PGA

for the 475-year return period in the analysis is 0.198 g (19.8% of gravity acceleration). This value concurs with literature [26]. The PGA for the 1000-year return period in the analysis is 0.252 g, which is the value used for the dam analysis. For the 5000-years return period, the PSA for $T = 0.25$ s is 0.928 g, which is similar to the deterministic PSA (1.00 g); this is because a probabilistic analysis for a large return period is unrealistic and often overestimated. In Fig. 6, the deterministic spectra obtained for four historical earthquakes, via two different attenuation relations, are shown. In the Spanish code, the PGA for this area is 0.17 g; however, in the full analysis, the soil with the greatest registered acceleration is 0.511 g, which is three times higher than the Spanish code.

4 Case study

4.1 The Rules dam on the Guadalfeo River

The structure of interest is a large, concrete, arch-gravity dam in the Granada province of southern Spain. This dam has a 620 m crown length and a 500-m radius. The maximum height of the vertical cantilever is 130.33 m (central black block in Fig. 7b), and the downstream and upstream slope faces are 1:0.60 and 1:0.18, respectively. The dam is made from 32 blocks. The seven dark grey blocks in the centre represent the spillway. The reservoir is shown in Fig. 7a [27]. The capacity and area for the maximum operating level of the reservoir are 117.07 Hm³ and 308
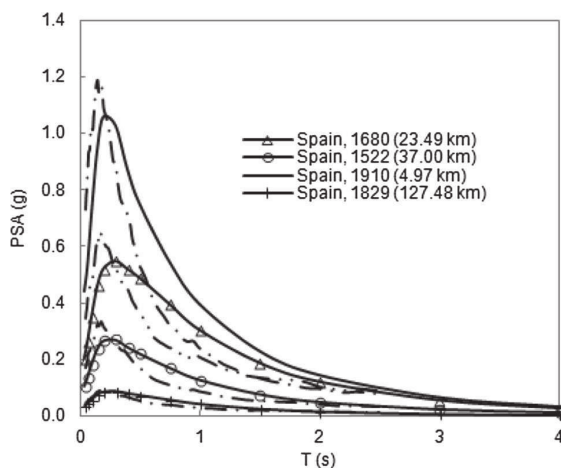

Fig. 6 Deterministic spectra of four records using SP96 and using Am05 (in dashed line). In the brackets, the estimated R_{jb} distance used in the Am05 equation is shown
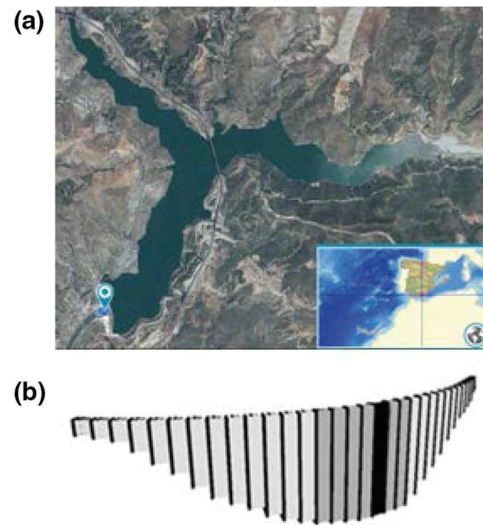

Fig. 7 Position of the Rules dam (36°51′35″ N, 3°29′43″ W) (**a**) and FEA 3D model (**b**)

Ha, respectively, whereas the area of the water basin is 1070 km².

4.2 Mathematical model

The numerical simulation was made using Finite Element Analysis (FEA) and the gravity method. The two- and three-dimensional FEA (Sap2000 software) [28] methods were used. The discretization of the 2D and 3D models are explained below.

In FEA (3D), the solid elements (32,980 elements) have a dimension of 3.00 m per 2.50 m, and there are 36,925 monolith joints. Those joints are necessary to analyse the nonlinear effects, such as concrete cracking and plastic hinges [29]. In the 3D model, the length of the block is 19.375 m. In FEA (2D), the solid elements (683 elements) have a dimension of 3.01 m per 2.79 m, and there are 765 joints. In the 2D model, the length of the block is 1 m. The solid element has eight nodes; each one has three degrees-of-freedom. In the gravity method (2D), the principal triangle of the central dam block has been considered. The height is 120 m, and the base is 93.6 m. The dam is divided into 48 lift joints with 2.5-m heights. The gravity method has been used only for the 2D analysis; it is based on rigid body equilibrium and on beam theory. The dam, via the 2D analysis, has been idealized as a triangular shape [30, 31] because the transverse behaviour is similar to a thick gravity dam with a large base thickness. The lift joints have homogeneous properties, and the loads are transferred to the foundation only by cantilever; therefore, it does not consider the arch-effect. The foundation

and abutments have rocky stratigraphic profiles; the values of the site geology refer to an average shear wave velocity over 750 m/s. Since the foundation is rocky, the base has been considered fixed, i.e., the direction displacements of all points of the base are constrained. The gravity method does not consider the dam-foundation interaction, and therefore, the constraints are not well-defined (it is enough to insert the foundation parameters, which is explained below). The loads present in the FEA include the dead load, the hydrostatic pressure and the hydrodynamic pressures. In the gravity method, in addition to the three loads, the seismic dead load and uplift load have been applied. In FEA, the hydrodynamic and hydrostatic pressures act normal to the face and are uniform for each solid.

The pseudo-hydrodynamic pressure occurs because the water is linearly compressible and irrotational. Furthermore, the internal viscosity of water is neglected, and the effects of waves at the free surface are omitted [32]. The hydrodynamic pressure of incompressible water (pressure independent of frequency) and the absorption effects of the reservoir bottom [33] have also been studied. In this example, the input data used are $E_c = 44.40$ GPa (modulus of elasticity of the concrete), $\gamma_c = 24$ kN/m³ (mass density of the concrete), $\nu_c = 0.20$ (Poisson's ratio of the concrete) and $\xi_d = 5\%$ (dam damping). In the FEA models, to consider the voids (e.g., galleries, drains and spillways) in the dam body, γ_c is set to 20.64 kN/m³, i.e., less than 14% of 24 kN/m³. This difference has been obtained from the ratio of the real weight to the model weight: $(3.6 \times 10^3 \ t)/(4.2 \times 10^3 \ t) = 0.86$. To consider the interaction between the substructures, e.g., dam–reservoir–foundation–sediments [34] and dam–abutments, the following data have been used: $E_f = 41.55$ GPa (modulus of elasticity of the foundation rock), $\gamma_f = 27.47$ kN/m³ (mass density of the foundation rock), $\nu_f = 0.33$ (Poisson's ratio of foundation rock), $\gamma_w = 9.81$ kN/m³ (mass density of water), $C_w = 1438$ m/s (velocity of pressure waves) and $\alpha_w = 0.41$ (wave reflection coefficient for reservoir bottom materials).

5 Results of the dynamic analysis

The recorded data must be carefully analyzed by performing the appropriate corrections and focusing on seismic demands [35, 36]. The controlling earthquakes have been used for this THA. By defining the significant durations [37] for each record, it is possible to select the most influential interval. Figure 8 shows the THA of the vertical stresses (σ_y) at the wall's heel of the dam's central block using three records; it shows the cases of empty and full reservoirs and both dynamic actions (seismic deadweight and hydrodynamics). In this case, the seismic deadweight includes the self-weight. In the analysis, there are slight differences between the analytical (normal stress) and the computational analysis (principal stress). The analytic pressure values are in accordance with those reported in the literature [38]. The principal stresses, due to the wall inclination, are obtained by software [39]. The full reservoir analysis demonstrates that the stresses are lower due to the hydrostatic and uplift negative stresses. However, during the seism, uplift pressures within the crack can be assumed to be zero, and therefore, the σ_y total increases. The constitutive law for compression and tension used for concrete is in accordance with the European Committee for Standardization [40]. The maximum tensile value adopted, which generates significant nonlinear plastic deformations, is $f_{ctd} = 1547$ kN/m² (horizontal dashed line in Figs. 8, 9). Other tensile strengths, which can be used for gravity dams with lower characteristics ($f_{ctd} = 960$ kN/m²), are shown in Figs. 8 and 9. For the unfavourable (unf.) full reservoir, when all forces have the same direction, the stresses exceed the ± 960 kN/m² value by 174 times in the heel and 558 in the toe. The stress analysis determines potential crack (the crack opens and closes during the earthquake) and plastic hinge formations. For each vibration, the stress analysis accumulates inelastic deformations [41], producing a hysteretic behaviour that depends on dissipated energy. Figure 9 shows the THA

Fig. 8 Dynamic stress at the heel of the wall (singular point in the upstream)
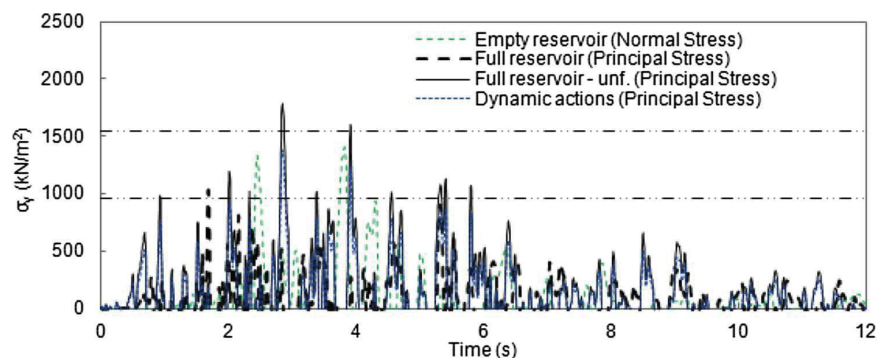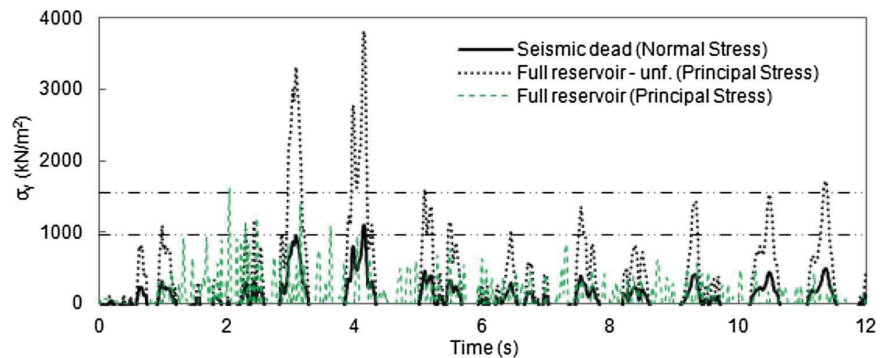
Fig. 9 Dynamic stress at the toe of the wall (singular point in the downstream)

of the stresses in the wall's toe of the dam's central block using two records. The seismic dead weight also includes the self-weight.

The structural analysis provided the following results: T_d is 0.284 s, the second dam period is 0.245 s, and the third dam period is 0.208 s. The first dam-reservoir period is 0.344 s, and the system's (dam-foundation-reservoir) fundamental period, T_s, is 0.393 s (the system damping, ξ_s, is 8.5%). The operating level considered is 113.00 m. The seismic dead weight and the hydrodynamic normal stresses, in relation to the maximum values calculated in this analysis, are less than 31.6% (at one-third of y) and 68.4% (at two-thirds of y) and 42.1% (at one-third of y) and 89.5% (at two-thirds of y), respectively. The y axis is zero in the bottom of the reservoir. The self-weight and hydrostatic horizontal stresses are -71.78 kN/m^2 (at the toe), -239.26 kN/m^2 (at the heel), -1028.24 kN/m^2 (at the toe), and -585.09 kN/m^2 (at the heel), respectively. Along the base of the dam, the seismic dead stresses increase, whereas the hydrostatic stresses decrease. The hydrodynamic and hydrostatic pressure effects and the sediment effects have been studied by other authors [42] and, therefore, are not shown here.

6 Conclusions

In this paper, the seismic risk of the Rules dam is evaluated. The possible maximum accelerations that can act against the dam's body are evaluated, and the dam's behaviour has been made explicit. The main conclusions are summarized as follows:

- The analysis has been performed in the site in which the dam is placed. The analysis carried out in this study shows that there are some differences in relation with the Zesis data. However, a precise study "ad hoc" is needed. Different values were only obtained in four zones ($\Delta\lambda_c$, Δb and $\Delta m_{,max}$ range between -0.31 and 0.23, -0.75 to 0.67, -0.2–1.7, respectively). The

seismic hazard is high and has a maximum moment magnitude of 6.8. The main differences are due to the recovered data and process uncertainties, e.g., the choice of the operations: homogenization, declustering and completeness.

- The PSHA and the DSHA have been used to define the design parameters. In the Spanish code, the PGA for the area is 0.17 g. In the PSHA, the PGA range is 6–135% higher than 0.17 g. In the DSHA, the range goes up to 200%. By considering the return period of the seismic action, for the no-collapse requirement of 1000 years, 0.25 g of ground acceleration has been calculated for the analysis. This study does not consider the site effects, e.g., amplification, topographic effects, and effect of foundation inhomogeneity [43]. This paper encourages the development of these issues in future research.

- The obtained system values are as follows: a fundamental period of 0.39 s and 8.5% damping. The system represents the interaction between the dam, foundation and water. In the heel, the increase due to dynamic action is 41.67% of the self-weight normal stress and 41.19% of the water principal stress. In the toe, the horizontal stress due to the hydrostatic action in the dam is 36% of the vertical stress. In the dynamic analysis, the maximum vertical principal stress is 3.8 MPa, while in the pseudo-static analysis—a rigid system with a period of vibration equal to zero—it is 2.6 MPa. An important number of inelastic deformations have been observed. The seismic input is obtained from a seismic hazard reanalysis. Since the structure was built (in 2003) before the modern seismogenic zone was created, these calculations and considerations may not be accurate since they were made in the original dam project.

References

1. Cornell CA (1968) Engineering seismic risk analysis. Bull Seismol Soc Am 58(5):1583–1606
2. Woo G (1996) Kernel estimation methods for seismic hazard area source modeling. Bull Seismol Soc Am 86(2):353–362
3. Gaspar-Escribano JM, Rivas-Medina A, Parra H, Cabañas L, Benito B, Ruiz Barajas S, Martínez Solares JM (2015) Uncertainty assessment for the seismic hazard map of Spain. Eng Geol 199:62–73
4. Faccioli E, Paolucci R (2005) Elementi di sismologia applicata all'ingeneria. Pitagora Editrice, Bologna
5. Comisión Permanente de Normas Sismorresistentes (2002) Norma de construcción sismorresistente: Parte general y edificación. Ministro de Fomento, Madrid
6. Gutenberg B, Richter CF (1944) Frequency of earthquakes in California. Bull Seismol Soc Am 34(4):185–188
7. Zhan Z (2017) Gutenberg-Richter law for deep earthquakes revisited: a dual-mechanism hypothesis. Earth Planet Sci Lett 461:1–7
8. IGME (2015) ZESIS: Base de Datos de Zonas Sismogénicas de la Península Ibérica y territorios de influencia para el cálculo de la peligrosidad sísmica en España. http://info.igme.es/zesis. Accessed June 2016
9. López Casado C, Sanz de Galdeano C, Delgado J, Peinado MA (1995) The b parameter in the Betic Cordillera, Rif and nearby sectors. Relations with the tectonics of the region. Tectonophysics 248:277–292
10. Instituto Geográfico Nacional (IGN) (2017). http://www.ign.es/web/ign/portal/sis-catalogo-terremotos. Accessed 14 June 2016
11. Instituto Andaluz de Geofísica (IAG) (2017). http://iagpds.ugr.es/
12. Sabetta F, Pugliese A (1996) Estimation of response spectra and simulation of nonstationary earthquake ground motions. Bull Seismol Soc Am 86(2):337–352
13. Ambraseys NN, Simpson KA, Bommer JJ (1996) Prediction of horizontal response spectra in Europe. Earthq Eng Struct Dyn 25:371–400. doi:10.1002/(SICI)1096-9845(199604)25:4<371::AID-EQE550>3.0.CO;2-A
14. Ambraseys NN, Douglas J, Sarma SK, Smit PM (2005) Equations for the estimation of strong ground motions from shallow crustal earthquakes using data from Europe and the Middle East: Horizontal peak ground acceleration and spectral acceleration. Bull Earthq Eng 3(1):1–53. https://doi.org/10.1007/s10518-005-0183-0
15. Berge-Thierry C, Cotton F, Scotti O (2003) New empirical response spectral attenuation laws for moderate European earthquakes. J Earthquake Eng 7(2):193–222. https://doi.org/10.1080/13632460309350446
16. Benito B, Gaspar-Escribano JM (2007) Ground motion characterization and seismic hazard assessment in Spain: context, problems and recent developments. J Seismolog 11:433–452. https://doi.org/10.1007/s10950-007-9063-1
17. Scordilis EM (2006) Empirical global relations converting M_s and m_b to moment magnitude. J Seismolog 10:225–236. https://doi.org/10.1007/s10950-006-9012-4
18. Benito MB, Navarro M, Vidal F, Gaspar-Escribano J, García-Rodríguez MJ, Martínez-Solares JM (2010) A new seismic hazard assessment in the region of Andalusia (Southern Spain). Bull Earthq Eng 8:739–766. https://doi.org/10.1007/s10518-010-9175-9
19. Cabañas L, Rivas-Medina A, Martínez-Solares JM, Gaspar-Escribano JM, Benito B, Antón R, Ruiz-Barajas S (2015) Relationships between M_w and other earthquake size parameters in the Spanish IGN seismic catalog. Pure Appl Geophys 172:2397–2410. https://doi.org/10.1007/s00024-014-1025-2
20. Gardner JK, Knopoff L (1974) Is the sequence of earthquakes in southern California, with aftershocks removed, Poissonian? Bull Seismol Soc Am 64(5):1363–1367
21. Ordaz M, Aguilar A, Arboleda J (2007) Crisis2007 (Version 5.4). Unam, Coyoacán
22. Sanz de Galdeano C, Peláez Montilla JA, López Casado C (2003) Seismic potential of the main active faults in the Granada basin (southern Spain). Pure Appl Geophys 160:1537–1556. https://doi.org/10.1007/s00024-003-2359-3
23. Luzi L, Puglia R, Russo E, ORFEUS WG5 (2016) Engineering Strong Motion Database, version 1.0. Istituto Nazionale di Geofis e Vulcanol Obs Res Facil Eur Seismol. doi:10.13127/ESM. http://esm.mi.ingv.it. Accessed 16 December 2016
24. Seismosignal (Version 4.0.0) (2010). Seismosoft Ltd, Pavia
25. García-Mayordomo J, Insua-Arévalo JM (2011) Seismic hazard assessment for the Itoiz dam site (Western Pyrenees, Sapin). Soil Dyn Earthq Eng 31:1051–1063. https://doi.org/10.1016/j.soildyn.2011.03.011
26. Gaspar-Escribano JM, Navarro M, Benito B, García-Jerez A, Vidal F (2010) From regional- to local-scale seismic hazard assessment: examples from Southern Spain. Bull Earthq Eng 8:1547–1567. https://doi.org/10.1007/s10518-010-9191-9
27. SNCZI-Inventario de Presas y Embalses (2017). http://sig.mapama.es/snczi/visor.html
28. Sap2000 (Version 16.0.0 Plus) (2013) Computers and Structures, Inc, California/New York
29. Durieux JH, Van Rensburg BWJ (2016) Development of a practical methodology for the analysis of gravity dams using the non-linear finite element method. J S Afr Inst Civil Eng 58(2):2–13
30. Khosravi S, Heydari MM (2013) Modelling of concrete gravity dam including dam-water-foundation rock interaction. World Appl Sci J 22(4):538–546. https://doi.org/10.5829/idosi.wasj.2013.22.04.551
31. Kaveh A, Ghaffarian R (2015) Shape optimization of arch dams with frequency constraints by enhanced charged system search algorithm and neural network. Int J Civil Eng 13(1):102–111. https://doi.org/10.22068/IJCE.13.1.102
32. Chakrabarti P, Chopra AK (1973) Earthquake analysis of gravity dams including hydrodynamic interaction. Earthq Eng Struct Dyn 2:143–160. https://doi.org/10.1002/eqe.4290020205
33. García F, Aznárez JJ, Padrón LA, Maeso O (2016) Relevance of the incidence angle of the seismic waves on the dynamic response of arch dams. Soil Dyn Earthq Eng 90:442–453
34. Tarinejad R, Pirboudaghi S (2015) Legendre spectral element method for seismic analysis of dam-reservoir- interaction. Int J Civil Eng 13(2):148–159. https://doi.org/10.22068/IJCE.13.2.148
35. Wang G, Wang Y, Lu W, Yan P, Zhou W, Chen M (2016) A general definition of integrated strong motion duration and its effect on seismic demands of concrete gravity dams. Eng Struct 125:481–493
36. Hariri-Ardebili MA, Mirzabozorg H, Kianoush R (2014) Comparative study of endurance time and time history methods in seismic analysis of high arch dams. Int J Civil Eng 12(2):219–236
37. Peláez JA, Delgado J, López Casado C (2005) A preliminary probabilistic seismic hazard assessment in terms of Arias intensity in southeastern Spain. Eng Geol 77:139–151. https://doi.org/10.1016/j.enggeo.2004.09.002

38. Millán MA, Young YL, Prévost JH (2002) The effects of reservoir geometry on the seismic response of gravity dams. Part 1: Analytical model. Earthq Eng Struct Dyn 00:1–6
39. Leclerc M, Léger P, Tinawi R (2004) Cadam (Version 1.4.14). CRSNG/Hydro-Québec/Alcan, Montréal
40. European Committee for Standardization (2004) Design of concrete structures. Part 1–1: general rules and rules for buildings. CEN, Brussels
41. Alembagheri M (2016) Earthquake damage estimation of concrete gravity dams using linear analysis and empirical failure criteria. Soil Dyn Earthq Eng 90:327–339
42. Zacchei E, Molina JL, LRF Brasil MR (2017) Seismic hazard and structural analysis of the concrete arch dam (Rules dam on Guadalfeo River). Procedia Eng 199:1332–1337. http://dx.doi.org/10.1016/j.proeng.2017.09.334
43. Joshi SG, Gupta ID, Murnal PB (2015) Analyzing the effect of foundation inhomogeneity on the seismic response of gravity dams. Int J Civil Struct Eng 6(1):11–24. https://doi.org/10.6088/ijcser.6002

ARTÍCULO 3

Nonlinear Degradation Analysis of Arch-Dam Blocks by using Deterministic and Probabilistic Seismic Input

Enrico Zacchei[1], José Luis Molina[1] and Reyolando M. L. R. F. Brasil[2]

[1]Higher Polytechnic School of Ávila, University of Salamanca (USAL), 50 Hornos Caleros, Spain

enricozacchei@usal.es

[2]Polytechnic School of São Paulo, University of São Paulo (USP), 380 Prof. Luciano Gualberto, Brazil

Abstract

This paper aims to define the non-linear response of arch-dam blocks. The plastic-degradation theory has been used to define the reduction of the elasto-plastic modulus during the hysteretic cycles. The parameters that are used to apply the model are obtained by literature and numerical analysis. In this sense, working with a reduction of the elasto-plastic modulus is useful to define the displacement of the structure. The seismic input has been obtained from probabilistic and deterministic seismic hazard analyses. For that, a series of several earthquakes have been chosen to perform the time-history analysis. The response of the structure blocks under four earthquakes has been made by using a step-by-step direct integration. An application to Rules Dam has been made to test the method.

1 Introduction

Due to an increasing demand for power and drinkable water, dams continue to be important structures for the population. The use of the impounding reservoir of the Rules Dam is for water storage, protection from floods and irrigation. In literature there are several case studies about seismic dams but only few of them are about arch dams which have suffered serious damage under intensive earthquake[1]. Consequently, there is not much scientific knowledge on types of cracking. In recent years, the nonlinear dynamic response of dams under earthquake actions, including cracking of the concrete, has attracted more researchers[1,2,3]. Some significant topics are, for example, the appropriate damping ratio for the concrete[4].

This paper is divided into three parts: definition of the seismic input where the dam is placed, definition of the hypothesis of the model, and analysis of the non-linear response. Definition of the seismic input is important because dams in southern Spain suffer from moderate to high earthquakes. The study of the model hypothesis is necessary for not under- or over-estimating the stresses, neglecting water compressibility, wave absorption at the reservoir boundary and foundation mass and damping.

The response of the structure blocks under four seisms was made by a non-linear seismic analysis using a step-by-step integration. Under cyclic loading, the mechanism of the stiffness degradation is difficult to define due to the formation of micro-cracks. Internal damage of structures inevitably lead to change of the structural dynamic parameters; as, for example, natural frequency, damping and vibration shapes. The softening and losing of the strength (compression and tension), in the broken regions under axial cyclic loadings, affect the seismic safety of the arch dam. The horizontal tensile stress, for example, produces cracks because the concrete tensile capacity is weak.

To carry out the non-linear analysis, the plasticity model has been used because it is rather simple to develop compared, for example, to the fracture mechanic model[5]. The former model defines the elastic-plastic modulus, whereas the latter defines the potential crack that depends on the softening curve, which is rather difficult to calculate.

A Finite Element Analysis (FEA) has also been carried out for an easy computation of the stresses of arch-dams. In 2-D analysis it is possible to consider a dam block as an equivalent simple oscillator because, during the motion, the mass is the most predominant parameter[6]. These approximations are generally useful for having a reference about the results because it is difficult to calculate satisfactorily the dam body's stress results and its foundation.

Finally, in 3-D analysis the interaction between the block vertical joints, dam-foundation and dam-water can be analysed. The spatial variations of the ground motion are not ignored. A strong intensity of the seism can produce damage to the entire structure or only to some parts of it. The damage mechanism can occur in the neck as well as, in the separation line between foundation and dam, in the singular points (heel and toe), in the vertical joints and discontinuity slopes. This mechanism is caused by several factors such as deflection of the crest, overturning, sliding and loss of the passive resistance of the rocky wedge.

2 Seismic Input

The seismic input has been obtained here from Probabilistic and Deterministic Seismic Hazard Analyses (P- and D-SHA)[7]. The P- and the D-SHA obtain the most probable occurrence of earthquakes and the most intense ones. The PSHA is calculated using Cornell method and it is developed in four steps: (i) identification and characterization of earthquake sources (http://info.igme.es/zesis/); (ii) characterization of the magnitude-recurrence distributions with the hypothesis of the Poisson process, which implies the Gutenberg and Richter law; (iii) evaluation of the ground motion where the Rules Dam is placed using attenuation equations[8,9]; and (iv) calculation of the hazard curves. The DSHA is developed in three steps: (i) selection of the historic earthquake, (ii) evaluation of the ground motion where the Rules Dam is placed using attenuation equations[8,10]; and (iii) calculation of spectra accelerations.

Both analyses are based on stochastic processes related to the standard deviation (margin of error), which is present in the attenuation equations. In the PSHA the standard deviation is equal to zero. Instead, in the DSHA, since it does not take into account the probability of occurrence (return period), it is convenient to consider the standard deviations – the standard deviation values used here are ± 0.26 for SP96 and ± 0.32 for Am96.

The historic earthquake chosen to be used for the DSHA is the event numbered 2877, which occurred in Spain on July 16th, 1910, having as its magnitude moment M_w 6.1 (= surface wave magnitude M_s 6.0) and its site-station epicentral distance of 6.82 km (http://www.ign.es).

This specific seismic analyses results help to choose a series of records with several different levels of intensity which are useful to carry out the nonlinear dynamic analysis of the structure. Four records have been chosen, i.e. Greece, 13/09/1986 (event name: GR-1986-0006); Italy, 26/09/1997 (event name: IT-1997-0006); Italy, 29/05/2012 (event name: IT-2010-0011) and Turkey, 1999 (TK-1999-0415) (esm.mi.ingv.it).

Figure 1 shows Pseudo Spectra Acceleration (PSA) obtained by probabilistic analysis and for the deterministic analysis, and the Turkey 1999 record. Table 1 shows some relevant values. The subscripts refer to the used attenuation equations, i.e. SP96[8], Am96[9] and Am05[10]. These values are in accordance to similar studies in literature[11,12].
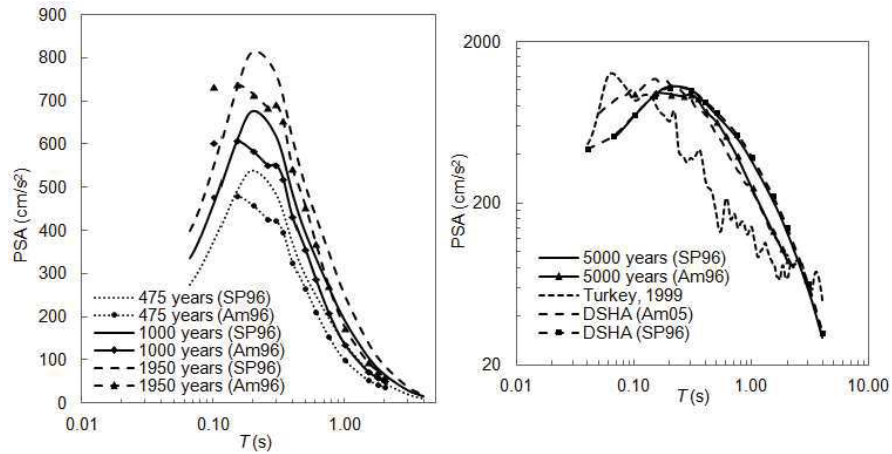
Fig. 1 PSA for different return periods (left and right), deterministic spectra (right) and Turkey 1999 record (right).

Table 1 Some results of the probabilistic and deterministic analysis.

		475 years	1000 years	1950 years	5000 years	-
PSHA*	$PSA|_{SP96}$ [cm/s^2]	463.63	593.10	729.17	962.37	-
	$PSA|_{Am96}$ [cm/s^2]	406.52	527.20	659.06	884.02	-
DSHA**	$PSA|_{SP96}$ [cm/s^2]	-	-	-	-	1038.32
	$PSA|_{Am05}$ [cm/s^2]	-	-	-	-	1165.84

*These PSA numbers are mean values of the structural period (T) 0.20–0.40 s (dam and system periods as well as the maximum PSA, which have been obtained in the analysis, are included in this interval).
**The DSHA|$_{Am05}$ is calculated for $T = 0.15$ s whereas the DSHA|$_{SP96}$ for $T = 0.2$ s.

3 Structural Data of the Model

Rules Dam is a concrete arch-gravity structure, situated in southern Spain in the Granada province. Table 2 shows data of the structure and reservoir.

Table 2 Data of the Rules Dam and the reservoir.

Crown length [m]	620.0
Radius [m]	500.0
Curvature angle in plan [°]	71.04
Bottom elevation of the higher vertical cantilever [m]	119.67
Top elevation of the higher vertical cantilever [m]	250.00
Mean higher of cantilevers [m]	74.783
Capacity of the reservoir for the maximum operating level [Hm^3]	117.07
Area of the reservoir for the maximum operating level [Ha]	308.0
Area of the water basin [km^2]	1070.0

Figure 2 shows the studied five blocks (in dark gray) (from the left to the right: 14A, 12A, 10A, 8A, 0A), the contact joints between blocks and the mode governing equations of the dam-foundation-water system (1), (2) and (3) that will be detailed below. The used coordinate references in the equations are: the x-axis is parallel to the flow direction and the Down-Stream (DS) direction is positive; the y-axis is parallel to the dam height direction and the upward is positive; the z-axis is perpendicular to the flow direction.

$$\frac{\partial \Pi}{\partial n}(\hat{n},t) + \rho_w \ddot{v}_g^n(t) + \rho_w \varphi_l^n(\hat{n}) \ddot{X}_l^n(t) = 0 \qquad (1)$$

$$\frac{\partial \Pi}{\partial n}(\hat{n},t) + \rho_w \ddot{v}_g^n(t) - \mu(\alpha_w, \tilde{v}_{b,w}) \frac{\partial \Pi}{\partial t}(\hat{n},t) = 0 \qquad (2)$$

$$\frac{\partial \Pi}{\partial n}(\hat{n},t) + \frac{1}{\tilde{v}_{b,w}} \frac{\partial \Pi}{\partial t}(\hat{n},t) = 0 \qquad (3)$$
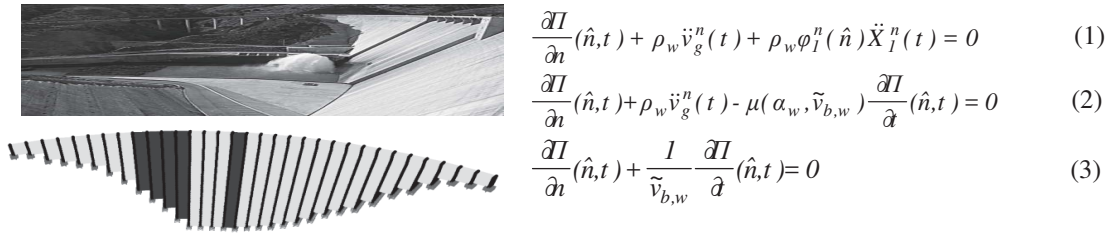
Fig. 2   Rules Dam DS photo (above), and (below) dam blocks, contact joint between blocks and foundation springs.

Table 3 shows data of the FEA of the dam (the SAP2000 software has been used for the modelling) and Table 4 shows data of the studied blocks.

Table 3 Data of FEA of the dam.

Number dam blocks	32
Number blocks of the central spillway	7
Mass density of the concrete [kN/m^3]*	20.64
Number of the solid elements (s_i)	32980
Number of the joints (j_i)	36925
j_i/s_i	1.119
Number of restraints defined (k_f^n)	3465
Number of angular divisions (Δz_i)	207
Number of radial divisions (Δx_i)	33.8
Number of vertical divisions (Δy_i)	47.4

*Considering the voids, the mass density of the concrete is 14% of 24 kN/m^3.

Arch-dams resists to the external forces thanks to the combination of the arches (horizontal elements) and the cantilevers (vertical elements). The interaction between arch and cantilever units is continuing: the load actions create movements that consist of n translational and n rotational components. Vertical y movements and rotations in vertical y planes might be negligible. The foundation has been considered rocky and mass-less. Mass-less foundation model takes into account only the elastic stiffness of the foundation medium, whereas the inertia and damping effects are neglected. Assuming the rigid foundation the stresses decrease because the soil rock model does not take into account the effects of the foundation: $k_f^n \to \infty$. The order of the magnitude of the rocky foundation stiffness is 10^9 kN/m, and for the mass-less foundation stiffness is 10^6 kN/m. Using the latter stiffness value the vertical stress due to the dam dead-weight increases 1.476 times (with $k_f^n = 0$ the vertical stresses are 147.69 times higher). The thrusts against the dam of the cross-canyon (abutments) excitation are been neglected since the behaviour is quasi-symmetrical.

Table 4 Data of the studied blocks.

Block	Elevation [m]	Height [m]	Base* [m]	Width [m]	Volume [m³]	Mass [10⁶ kg]	Equivalent Period [s]	Equivalent Inertia [m⁴]
14A	172.43	77.58	60.51	19.51	45784.76	109.883	0.193	24148.874
12A	158.54	91.46	71.34	19.51	63638.62	152.733	0.228	39572.786
10A	144.62	105.38	82.20	19.51	84487.75	202.771	0.262	60534.939
8A	128.82	121.18	94.52	19.51	111729.52	268.151	0.302	92059.239
0A	119.67	130.33	101.66	18.90	125203.13	300.488	0.324	110946.542

*The base is calculated considering a triangular dam shape with DS and Up-Stream (US) slope faces of 1:0.60 and 1:0.18, respectively.

4 Hypotheses of the Model

The hydraulic hypothesis[13,14] of the two- and three-dimensional (x,y,z) analyses are shown in this section. The system – governed by second order differential equations – is composed by the concrete dam, which impounds a reservoir (constant water depth), and the horizontal rigid rock. The hydrodynamic pressures are generated by horizontal motion of the dam semi-vertical US-face and by vertical motion of the horizontal reservoir bottom. Assuming water as linearly compressible and neglecting its internal viscosity and low amplitude, the irrotational motion of the water is governed by the wave equation. The normal pressure gradient of the hydrodynamic acoustic pressure $\Pi(x,y,z,t)$, at the vertical US-face of the dam, is proportional to the total acceleration of the boundary condition by (1). The used approach is the Eulerian method because in structures the variables are the displacements, while in fluids they are the pressures. In (1), ρ_w is the density of the water (the subscript w refers to the water); $\ddot{v}_g^n(t)$ is the ground acceleration in n-direction; $\varphi_1^n(\hat{n})$ is the component of the displacement in the dam 1st-mode natural vibration with an empty reservoir, and $\ddot{X}_1^n(t)$ is the modal coordinate that is associated to 1st-mode vibration. In (1), the second part represents the rigid pressures, whereas the third part represents the flexible pressure.

Considering only the vertically propagation waves due to the hydrodynamic pressure against the reservoir base, the boundary condition at the reservoir bottom is defined by (2). The fluid-foundation interaction has been shown in (2); where $\tilde{v}_{b,w}$ stands for the speed of water compressive wave, α_w is the wave reflection coefficient, $\mu = \rho_w/(\rho_f\,\tilde{v}_{b,f})$, $\tilde{v}_{b,f} = \sqrt{(E_f/\rho_f)}$, E_f is the Young's modulus of the foundation and ρ_f is the density of the foundation medium. For a rigid foundation $\tilde{v}_{b,f} = \infty$ and $\mu = 0$. Third term in (2) represents the modification of the vertical acceleration, i.e. $\ddot{v}_g^y(t)$ in the second term, which depends on the interaction between the fluid and flexible semi-infinite foundation. Since the pressure in the third term depends on the time t, the reservoir bottom produces a damping effect due to the radiated energy by means of the refraction of the waves in the foundation. The refracted waves can be dilatational (tensile or compressive deformations) and rotational (shear deformations). The other pressure waves are reflected in the water medium (in US-direction a part of the energy is lost). Since that the foundation is considered axially flexible with infinite length and infinitesimal width, only refracted waves are downward vertical waves. The hydrodynamic pressures have been calculated using $\alpha_w = 0.85$ that is the ratio of the amplitude of the reflected hydrodynamic wave and the amplitude of the vertical propagating wave incident on the bottom; it depends on the angle of incidence, sediment mass density, sound velocity in sediment, sediment layer depth and acoustic

impedance ($1/\mu$): dynamic stiffness between the layer of the reservoir and the layer of the rock (interface complex forces in the frequency domain between both layers). When $\alpha_w = 1$ ($\mu = 0$) the pressure has the same values of the hydrodynamic pressure for water compressible. When $\omega_{1,w} < 2\omega_{1,d}$ it is necessary an elaborated analysis of α_w. In this study $\omega_{1,w}/\omega_{1,d} = 0.8907$. For high dams a several analysis based on different values of the α_w is always required. For $\alpha_w = 0.85$ (i.e. the waves are mainly reflected in the water, 85%, and partially transmitted into the substrate, 15%) the maximum horizontal hydrodynamic pressure is 0.83 lesser than the maximum horizontal hydrodynamic pressure for $\alpha_w = 0.41$. Usually, it is possible to adopt $\alpha_w \approx 0.8$[15]. Neglecting the water superficial waves, the boundary condition at the free surface of the reservoir is: $\Pi(\hat{n},t)= 0$.

The hydrodynamic pressure satisfies the radiation condition in the US-direction (for infinity or semi-infinity length) by (3). The normal vector $\hat{n}$ refers, in all equations, to the interface of the considered boundary. To consider the ground acceleration in the circular frequency (ω) domain, the wave equation becomes the Helmholtz equation. When the interaction between the dam and the impounded water needs a solution in the frequency domain the water must be considered compressible. The described pressures are valid to calculate the excitation in the horizontal and vertical direction for rigid or flexible dams. In this study, only the effect due to the horizontal acceleration has been studied.

The foundation should be analyzed under the assumptions of anisotropy and nonlinear behavior for the rock, including the wave equations, but it is almost-impossible to take in account all rock discontinuities because geological data of the rock layers are not usually available. In the 3-D model the foundation can be defined by the rock and mass-less linear model.

Because of the complexity in the global analysis, divided substructure methods are preferred for the seismic analysis of dams. The three-system liquid-dam-rock can be divided in two parts: dam-foundation and dam-water. The equation of the motion for the dam-foundation system, in the n-direction, is[16]:

$$[M]\{\ddot{v}(t)\}+[C]\{\dot{v}(t)\}+[K]\{v(t)\}= -[M]\{\ddot{v}_g(t)\}+\{\Gamma(t)\} \tag{4}$$

in which M is the mass matrix, C is the damping matrix and K is the stiffness matrix. The displacement $v(t)$, velocity $\dot{v}(t)$ and acceleration $\ddot{v}(t)$ are the relative vectors to the soil base. The equation (4) represents the assembled system of two substructures where the foundation is idealized as a continuum. The first and second line of (4) are, respectively (the subscripts f refers to the foundation, whereas d refers to the dam):

$$m_d\ddot{v}_d(t)+(c_d+c_f)\dot{v}_d(t)-c_f\dot{v}_f(t)+(k_d+k_f)v_d(t)-k_fv_f(t)= -m_d\ddot{v}_g(t) \tag{5}$$

$$m_f\ddot{v}_f(t)-c_f\dot{v}_d(t)+c_f\dot{v}_f(t)-k_fv_d(t)+k_fv_f(t)= -m_f\ddot{v}_g(t)+\Gamma_f(t) \tag{6}$$

with $\Gamma_f(t)= c_{df}(\dot{v}_{df}(t)-\dot{v}_f(t))+k_{df}(v_{df}(t)-v_f(t))$, which is the interaction force between dam-foundation. The equation of the motion for the dam-water (not matrix system) is:

$$m_d\ddot{v}_d(t)+c_d\dot{v}_d(t)+k_dv_d(t)= -m_d\ddot{v}_g(t)+\Phi_w(t) \tag{7}$$

where $\Phi_w(t)$ is the exerted nodal force on the wall due to the hydrodynamic pressure. It is possible to think this force as an "elastic" force of the dam-rock-water system:

$$\Phi_{dw}(t) \equiv m_{dw}\ddot{\Pi}_e(t) + c_{dw}\dot{\Pi}_e(t) \tag{8}$$

in which, in a system assembled of two substructures, idealizing the water as a continuum, is:

$$k_{dw}(v_{dw}(t) - v_w(t)) \equiv \Phi_w(t) + c_{dw}(\dot{v}_{dw}(t) - \dot{v}_w(t)) \tag{9}.$$

Equation (8) has been obtained from discretization of the wave equation[17] where $\Pi_e(t)$ is the nodal pressure vector. The introduction of this variable is more consistent to study the fluid behaviour: usually, the response of the fluids is measured in terms of velocity or pressure, not in terms of displacement as (9).

5 Non-linear Seismic Analysis

During the vibration, a part of energy is dissipated irreversibly via structural instability, plasticity and creep; whereas the other part of the energy is stored via elastic strain energy which can be reused by the structure. The structural mechanical properties change during the analysis; in this sense, the stiffness and strength have a systematically decrement. The used non-linear model is based on the combination of plasticity theory[18] and damage mechanism. The criteria are: (i) Modified Mohr-Coulomb[19] (MMC) yield criterion, (ii) associated flow rule and (iii) softening curve. Flow rule describes the increment of plastic strain and, when the concrete is subject to severe inelastic state, the plastic distortion changes the concrete volume. Flow rule is called "associated" when the plastic potential is equal to yield function. The MMC criterium determines the stress when yielding occurs and regards the total damage to be equal only to the cohesion. The evolution of the yield branch (softening) is controlled by the cohesion curve which justifies the MMC choice. MMC is a function of the uniaxial stress component and considers the isotropic homogeneous material. However, it is worth to note that the failure depends more on the heterogeneous behaviour of the material.

The Plastic-Damage (PD) model, taking into account the stiffness degradation, is more appropriate to analyze the crack and failure of the concrete arch dams. The plastic stiffness considers a single variable, i.e. the tensile damage factor d_t. It varies from 0 (undamaged elastic material) to 1 (fully damaged material)[6]. In this study we have also considered that, during the load cycles, the slope of the elastic modulus ($E_{d,ei}$) decreases, therefore reloading is simulated by non-parallel lines to the initial slope of $E_{d,e0}$ (initial elastic modulus). However, the elastic modulus is underestimated because the recovery during the unloading phase has not been considered. The plastic stiffness is defined by $E_{d,ei}(1 - d_t)(1 - d_c)$. The compression damage factor has been considered $d_c = 0$ because the focus of the current work is only to study the concrete tensile behaviour. These two variables, d_t and d_c, aim at two distinct phenomena (cracking and crushing) that usually occur in the concrete under cyclic loadings. In this study, four idealized hysteretic cycles step-by-step have been considered: $\{E_{d,ei}|\ i = 1,2,3,4\}$. The exponential and linear Tension Softening Curve (TSC) has been used (see Fig. 3 (left)). Table 5 shows the concrete parameters which are obtained from iterative analyses supported by literature[4,5,6,20].

Table 5 Concrete parameters.

Tensile strength (f_t) [MPa]	2.73
Compressive strength (f_c) [MPa]	47.5
Initial elastic modulus ($E_{d,e0}$) [GPa]	1.2 x 37 = 44.40 GPa[7,21]
Poisson's ratio of the dam (v_d)	0.19*
Tension specific fracture energy (G_t) [N/m]	113.06
Characteristic micro-crack openings that propagate through the aggregates (w_c) [μm]	240.51
Crack band width of the fracture (l_c) [m]	0.45
Size of the element which models l_c for the linear analysis (h_0) [m]	1.35
Effective crack length (a_c) [m]	0.484**
Limit dynamic tensile strain (ε_{lt}) [μm]	165.87**

*Poisson's ratio of the dam usually ranges 0.15-0.25.
**The effective crack length has been estimated using data from literature[22,23]. The limit dynamic tensile strain, in accordance to literature[1,15].

To define ε_{lt} the characteristic length is been assumed 0.50 m, which represents the side of an equivalent cube of the volume of the 3-D solid element[15]: it can be utilized to study the crack phenomenon using only the mesh in FEA.

Figure 3 (left) shows the exponential and linear (dashed line) TSC. The filled area is the G_t/1.354. The G_t has been increased by experimental value in literature as already mentioned. The area under the stress line overestimates the tension softening curve of 2.9. Figure 3 (middle) shows the blocks of the dam during construction.
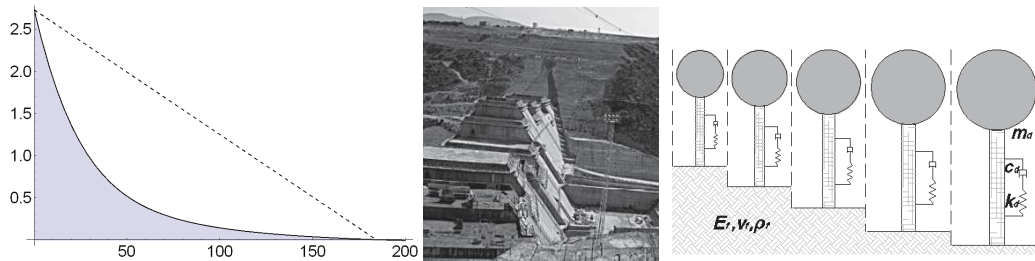

Fig. 3   Simple oscillators of the model by AutoCAD©software (from left to right: 14A, 12A, 10A, 8A, 0A) (right); blocks of the dam during construction (middle); exponential and linear TSC (left). TSC curves define the tensile strength (in MPa) vs. crack opening (μm) with the range 0-2.73 and 0-240.51, respectively.

In Fig. 3 (middle) it is possible to note that the blocks are constructed in different stage, changing the distribution of the stresses step-by-step. However, since the most important weight is the dead-weight, the construction in different stage does not influence much the final configuration of the stresses (except the variation of the temperature). In Fig. 3 (right) the oscillators of the five analyzed blocks and the matrix coefficients are shown – in (4) the matrix *M*, *C* and *K* are defined by matrix coefficients *m*, *c* and *k*, respectively. The oscillators are scaled each other in accordance to real height

(see Table 4): the relation between 14A and 0A (Fig. 3 (right)), is 1.679. The foundation rock parameters have also been shown: E_f = 41.55 GPa, ρ_f = 2.8 x 10^3 kg/m³, v_f = 0.31 (Poisson's ratio of the foundation).

6 Results and Conclusions

Time-history (TH) continuum approach by Wolfram Mathematica has been made. Each block has been considered as a simple oscillator, therefore the relation, considering the displacement in the top, between the stiffness and modulus is known. The increase of the dynamic loads in respect to the static loads has been taken into account considering the increase of the stiffness. It is also possible, and more convenient, to consider this increasing by a dynamic magnification factor to the elastic modulus (e.g., see coefficient used to define $E_{d,e0}$ in the Table 5). Due to around 10 m of the dam being fixed in the foundation and the modal participating mass ratio for the first three modes in the three directions being 83.7%, the dynamic mass has been assumed 90% of the static mass. The used dam damping ξ_d is 5% and it is constant during the analysis. The foundation hysteretic damping is 10%. The system (dam-foundation-reservoir) damping is 8.5%. The equivalent stiffness is obtained from equivalent inertia (see Table 4), which depends on the mass. The participating mass of the dam fundamental mode in the three directions is 45.1%; from this value the estimated coefficient that reduces the inertia is 0.03182.

Figures 4–5 show linear and non-linear response. The suggested unacceptable ultimate displacements[24,25] v_{ult} are: 0.13 m, 0.12 m, 0.10 m, 0.09 m and 0.07 m for the blocks 0A, 8A, 10A, 12A and 14A, respectively. Consist to the literature[3,6], the acceptable elastic displacement is v_{el} = v_{ult}/4. Both displacements, v_{ult} and v_{el}, are indicated in Figs. 4–5 by horizontal dashed lines.

In Figs. 4–5, the gray filled area represents the disadvantage that the structure has in the plastic state. The portion of the gray filled area that exceeds v_{el} represents the permanent deformation, whereas the portion of the gray filled area that exceeds v_{ult} represents the damage.
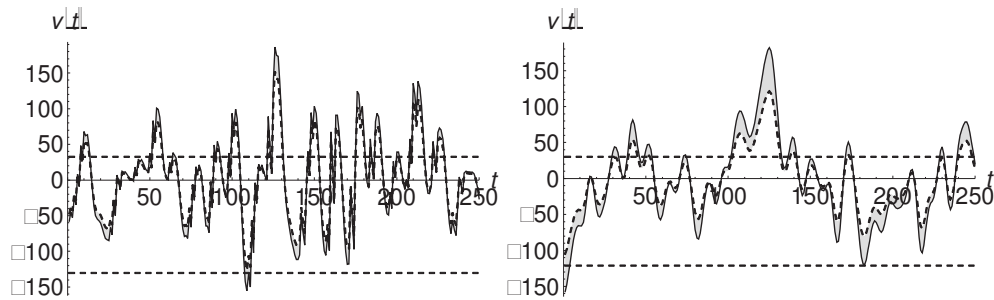

Fig. 4   Nonlinear and linear (dashed curve) TH analysis of the block 0A (left) and of the block 8A (right). The displacement is in mm.
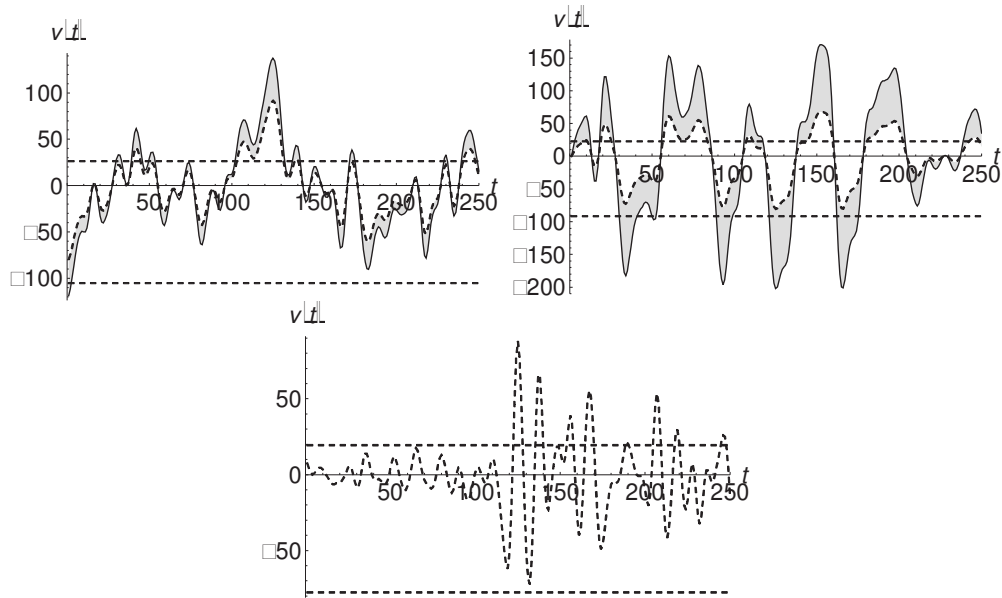
Fig. 5   Nonlinear and linear (dashed curve) TH analysis of the block 10A (left), 12A (right) and 14A (below). The displacement is in mm.

In the nonlinear analysis the gradually descending acceleration values have been considered, i.e. for the first cycle we use the acceleration with the higher value whereas for the fourth cycle we use the acceleration with the lower value. The idea is to simulate a strong earthquake and then three relevant after-shocks.

The hydrostatic and hydrodynamic forces have not been considered: they are about 2.49% and 0.52% of the pseudo-dynamic seismic force of the dam, respectively.

The seismic events described in previous section have been recorded by a number of seismic stations. The acceleration peaks in the TH analyses are: 346.28 cm/s^2 (Turkey, 1999), 242.83 cm/s^2 (Greece, 13/09/1986), 162.08 cm/s^2 (Italy, 29/05/2012) and 93.49 cm/s^2 (Italy, 26/09/1997). The difference between 346.28 cm/s^2 and the maximum value 5000 shown in Fig. 1 (right) is due to the fact that the values were recorded from different seismic stations.

The time scale in Figs. 4 and 5 is "virtual" since only a portion of 250 points with a time interval of 1.25 s ($\Delta t = 1.25/250 = 0.005$) of the four accelerograms have been taken. These intervals contain the four acceleration peaks. This interval comprises only a part of the complete TH, therefore some responses have a different initial drift. The axis of abscissa in Figs. 4 and 5 corresponds to the set: $\{v_i(t_j) \mid \forall v_i \in R, \forall t_j \in N, i \in R, j = (0,1,2,...,250)\}$.

In Table 6 the non-linear response of the five blocks is shown, where the $E_{d,ep}$ is the dam elasto-plastic modulus, $v_{el,max}$ and $v_{ep,max}$ are the maximum elastic displacement and maximum elasto-plastic displacement, respectively. The estimated greater unacceptable ultimate displacements[24,25] v_{ult} is 0.13 m. For displacements over 2 x 0.13 = 0.26 m = 260 mm, it has been considered that the structure might suffer severe damage (= sd).

Table 6 Non-linear analysis results. The displacement is in mm.

	$E_{d,ep}$ = 35.52 GPa		$E_{d,ep}$ = 20.25 GPa		$E_{d,ep}$ = 7.69 GPa		$E_{d,ep}$ = 1.46 GPa	
	$v_{el,\ max}$	$v_{ep,\ max}$	$v_{el,\ max}$	$v_{ep,\ max}$	$v_{el,\ max}$	$v_{ep,\ max}$	$v_{el,\ max}$	$v_{ep,\ max}$
0A	151.652	186.409	140.204	210.469	-163.666*	sd	sd	sd
8A	131.114	161.164	121.217	181.965	-141.501*	sd	sd	sd
10A	99.146	121.870	91.662	137.599	-107.001*	-268.461*	162.065	sd
12A	74.680	91.796	69.042	103.643	-80.596*	-202.212*	122.072	sd
14A	53.728	66.042	49.672	74.566	-57.984*	-145.408*	87.824	sd

*The absolute value must be considered. The negative values are consistent with the TH in Figs. 4 and 5.

In Table 7 working accumulation in terms of the displacement, v_{acc}, that exceeds v_{el} and v_{ult}, is shown. The former represents the accumulation of the plastic deformation and the latter represents the accumulation of the cracks. $\overline{x}$ is the mean value of the accumulation sums (amount of damage) of the considered cycle. The standard deviation σ is calculated by all the accumulations of the four cycles.

Finally the 3-D post-seismic analyses by FEA have been made considering the displacement due to hydrostatic actions for the full reservoir. Considering $E_{d,ep}$ = 1.46 GPa and v_c = 0.15 the maximum displacement in the DS direction of the whole dam is 67.179 mm. This displacement is not very large due to fact that the curvature of the arch dams produces greater stiffness (in the pre-seismic phase, the whole dam displacement is 13.77 mm).

Table 7 Non-linear accumulations of the displacements (in mm).

	v_{acc} {v_{el}} for $E_{d,ep}$ (GPa)				$\overline{x}$	σ	v_{acc} {v_{ult}} for $E_{d,ep}$ (GPa)
	35.52	20.25	7.69	1.46			20.25
0A	2043.514	4099.721	-	-	3071.617	±12.095	1002.972
8A	1723.265	3505.312	-	-	2614.288	±10.423	631.495
10A	1237.635	2542.294	16030.540	-	6603.490	±40.252	410.842
12A	905.991	1808.057	12023.073	-	4912.373	±30.590	166.170
14A	612.915	1171.511	8608.578	-	3464.334	±22.260	0

The decrease of the elastic-plastic modulus can be seen as an increase of the dam flexibility in terms of the vibration period (in 3-D analysis the reduction of vibration period is 4.93).

7 Acknowledgements

References

[1] Omidi, O. and Lofti, V., Seismic plastic-damage analysis of mass concrete blocks in arch dams including contraction and peripheral joints, *Soil Dynamics and Earthquake Engineering,* vol. 95, pp. 118–137, 2017.

[2] Zhang, Q. L., Wang, F., Gan, X. Q. and Li, B., A field investigation into penetration cracks close to dam-to-pier interfaces and numerical analysis, *Engineering Failure Analysis,* vol. 57, pp. 188–201, 2015.

[3] Alembagheri, M., Earthquake damage estimation of concrete gravity dams using linear analysis and empirical failure criteria, *Soil Dynamics and Earthquake Engineering,* vol. 90, pp. 327–339, 2016.

[4] Omidi, O., Lotfi, V. and Valliappan, S., Plastic-damage analysis of Koyna dam in different damping mechanisms with dam-water interaction, *15th World Conference on Earthquake Engineering, WCEE 2012,* Lisbon, Portugal, 24–28 September, 2012.

[5] Guanglun, W., Pekau, O. A., Chuhan, Z. and Shaomin, W., Seismic fracture analysis of concrete gravity dams based on nonlinear fracture mechanics, *Engineering Fracture Mechanics,* vol. 65, pp. 67–87, 2000.

[6] Wang, J. T., Jin, A. Y., Du, X. L. and Wu, M. X, Scatter of dynamic response and damage of an arch dam subjected to artificial earthquake accelerograms, *Soil Dynamics and Earthquake Engineering,* vol. 87, pp. 93–100, 2016.

[7] Zacchei, E., Molina, J. L. and L. R. F. Brasil, M. R., Seismic hazard assessment of arch dams via dynamic modelling: an application to the Rules Dam in Granada, SE Spain, *International Journal of Civil Engineering*, pp. 1–10, 2017.

[8] Sabetta, F. and Pugliese, A., Estimation of response spectra and simulation of nonstationary earthquake ground motions, *Bulletin of the Seismological Society of America,* vol. 86, pp. 337–352, 1996.

[9] Ambraseys, N. N., Simpson, K. A. and Bommer, J. J., Prediction of horizontal response spectra in Europe, *Earthquake Engineering and Structural Dynamics,* vol. 25, pp. 371–400, 1996.

[10] Ambraseys, N. N., Douglas, J., Sarma, S. K. and Smit, P. M., Equations for the estimation of strong ground motions from shallow crustal earthquakes using data from Europe and the Middle East: Horizontal peak ground acceleration and spectral acceleration, *Bulletin of Earthquake Engineering,* vol. 3, pp. 1–53, 2005.

[11] Gaspar-Escribano, J. M., Navarro, M., Benito, B., García-Jerez, A. and Vidal, F., From regional- to local-scale seismic hazard assessment: examples from Southern Spain, *Bulletin of Earthquake Engineering*, vol. 8, pp. 1547–1567, 2010.

[12] Benito, M. B., Navarro, M., Vidal, F., Gaspar-Escribano, J., García-Rodríguez, M. J. and Martínez-Solares, J. M., A new seismic hazard assessment in the region of Andalusia (Southern Spain), *Bulletin of Earthquake Engineering*, vol. 8, pp. 739–766, 2010.

[13] Fenves, G. and Chopra, A. K., Effects of reservoir bottom absorption on earthquake response of concrete gravity dams, *Earthquake Engineering and Structural Dynamics,* vol. 11, pp. 809–829, 1983.

[14] Demirel, E., Numerical simulation of earthquake excited dam-reservoirs with irregular geometries using an immersed boundary method, *Soil Dynamics and Earthquake Engineering,* vol. 73, pp. 80–90, 2015.

[15] Mirzabozorg, H., Varmazyari, M. and Ghaemian, M., Dam-reservoir-massed foundation system and travelling wave along reservoir bottom, *Soil Dynamics and Earthquake Engineering,* vol. 30, pp. 746–756, 2010.

[16] Chakrabarti, P. and Chopra, A. K., Earthquake analysis of gravity dams including hydrodynamic interaction, *Earthquake Engineering and Structural Dynamics,* vol. 2, pp. 143–160, 1973.

[17] Seyedpoor, S. M., Salajegheh, J. and Salajegheh, E., Shape optimal design of arch dams including dam-water-foundation rock interaction using a grading strategy and approximation concepts, *Applied Mathematical Modelling,* vol. 34, pp. 1149–1163, 2010.

[18] Lubliner, J., Oliver, J., Oller, S. and Oñate, E., A plastic-damage model for concrete, *International Journal of Solids and Structures,* vol. 25, pp. 299–326, 1989.

[19] Oñate, E., Oller, S., Oliver, J. and Lubliner, J., A constitutive model for cracking of concrete based on the incremental theory of plasticity, *Engineering Computations,* vol. 5, pp. 309–319, 1988.

[20] Chen, H. H. and Su, R. K. L., Tension softening curves of plain concrete, *Construction and Building Materials,* vol. 44, pp. 440–451, 2013.

[21] U. S. Army Corps of Engineers (USACE), *Arch dam design*, Manual No. 1110-2-2201, 1994.

[22] Guan, J., Li, Q., Wu, Z., Zhao, S., Dong, W. and Zhou, S., Minimum specimen size for fracture parameters of site-casting dam concrete, *Construction and Building Materials,* vol. 93, pp. 973–982, 2015.

[23] Li, Q., Guan, J., Wu, Z., Dong, W. and Zhou, S., Equivalent maturity for ambient temperature effect on fracture parameters of site-casting dam concrete, *Construction and Building Materials,* vol. 120, pp. 293–308, 2016.

[24] Hariri-Ardebili, M. A., Seyed-Kolbadi, S. M. and Kianoush, M. R., FEM-based parametric analysis of a typical gravity dam considering input excitation mechanism, *Soil Dynamics and Earthquake Engineering,* vol. 84, pp. 22–43, 2016.

[25] Hariri-Ardebili, M. A. and Saouma, V., Quantitative failure metric for gravity dams, *Earthquake Engineering and Structural Dynamics,* vol. 44, pp. 461–480, 2015.

30 December 2017

Professor Enrico Zacchei   E-mail: *enricozacchei@gmail.com*

Higher Polytechnic School of Ávila

University of Salamanca

50 Hornos Caleros

Spain

Dear Professor Enrico Zacchei,

Title: JVET/CW/896 Nonlinear Degradation Analysis of Arch-Dam Blocks by using
             Deterministic and Probabilistic Seismic Input

Author(s):   Enrico Zacchei, José Luis Molina and Reyolando M.L.R.F. Brasil

Having considered your revision, I am pleased to inform you that your revised manuscript submitted to *Journal of Vibration Engineering & Technologies* has been accepted for publication.

Thank you for your interest and contribution to the journal.

Yours sincerely,

C.W. Lim

FASME, FASCE, F.EMI, FHKIE, FISEAM, RPE

Associate Editor, Asia Pacific Region

Journal of Vibration Engineering & Technologies